5-2010

Developing Chitosan-based Biomaterials for Brain Repair and Neuroprosthetics

Zheng Cao
Department of Materials Science and Engineering, UTK, zcao1@utk.edu

To the Graduate Council:

I am submitting herewith a thesis written by Zheng Cao entitled "Developing Chitosan-based Biomaterials for Brain Repair and Neuroprosthetics." I have examined the final electronic copy of this thesis for form and content and recommend that it be accepted in partial fulfillment of the requirements for the degree of Master of Science, with a major in Polymer Engineering.

Wei He, Major Professor

We have read this thesis and recommend its acceptance:

Roberto S. Benson, Kevin M. Kit

Accepted for the Council:
Dixie L. Thompson

Vice Provost and Dean of the Graduate School

(Original signatures are on file with official student records.)

To the Graduate Council:

I am submitting herewith a thesis written by Zheng Cao entitled "Developing Chitosan-based Biomaterials for Brain Repair and Neuroprosthetics". I have examined the final electronic copy of this thesis for form and content, and recommend that it be accepted in partial fulfillment of the requirements for the degree of Master of Science, with a major in Polymer Engineering.

Wei He

We have read this thesis
and recommend its acceptance:

Roberto S. Benson

Kevin M. Kit

Accepted for the Council:

Carolyn R. Hodges

Vice Provost and
Dean of the Graduate School

Developing Chitosan-based Biomaterials for Brain Repair and Neuroprosthetics

A Thesis
Presented for the
Master of Science Degree
The University of Tennessee, Knoxville

Zheng Cao
May 2010

ACKNOWLEDGEMENTS

I would like to express my sincere thanks to my advisor, Dr. Wei He, for her guidance and support throughout my graduate studies. I gratefully acknowledge Dr. Roberto S. Benson and Dr. Kevin M. Kit for serving on my committee and mentoring me in the field of polymer engineering. I would like to thank Dr. Judy Grizzle, Dr. John Dunlap, Gregory Jones, Dr. Federico Harte, Dr. Michael Smith, Dr. Svetlana Zivanovic, Dr. Mingjun Zhang, and their students for the generous support on my research. I also want to thank my fellow labmates, Yu Cao, Jonathan Page, and Kaan Serpersu for being great helpers in research and friends in daily life. Finally, to my family and friends, without your understanding and support none of this would have been possible.

ABSTRACT

Chitosan is widely investigated for biomedical applications due to its excellent properties, such as biocompatibility, biodegradability, bioadhesivity, antibacterial, etc. In the field of neural engineering, it has been extensively studied in forms of film and hydrogel, and has been used as scaffolds for nerve regeneration in the peripheral nervous system and spinal cord. One of the main issues in neural engineering is the incapability of neuron to attach on biomaterials. The present study, from a new aspect, aims to take advantage of the bio-adhesive property of chitosan to develop chitosan-based materials for neural engineering, specifically in the fields of brain repair and neuroprosthetics. Neuronal responses to the developed biomaterials will also be investigated and discussed.

In the first part of this study (Chapter II), chitosan was blended with a well-studied hydrogel material (agarose) to form a simply prepared hydrogel system. The stiffness of the agarose gel was maintained despite the inclusion of chitosan. The structure of the blended hydrogels was characterized by light microscopy and scanning electron microscopy. In vitro cell studies revealed the capability of chitosan to promote neuron adhesion. The concentration of chitosan in the hydrogel had great influence on neurite extension. An optimum range of chitosan concentration in agarose hydrogel, to enhance neuron attachment and neurite extension, was identified based on the results. A "steric hindrance" effect of chitosan was proposed, which explains the origin of the morphological differences of neurons in the blended gels as well as the influence of the physical environment on neuron adhesion and neurite outgrowth. This chitosan-agarose (C-A) hydrogel system and its multi-functionality allow for applications of simply prepared agarose-based hydrogels for brain tissue repair.

In the second part of this study (Chapter III), chitosan was blended with graphene to form a series of graphene-chitosan (G-C) nanocomposites for potential neural interface applications. Both substrate-supported coatings and free standing films could be prepared by air evaporation of precursor solutions. The electrical conductivity of graphene was maintained after the addition of chitosan, which is non-conductive. The surface characteristic of the films was sensitively dependent on film composition, and in turn,

influenced neuron adhesion and neurite extension. Biological studies showed good cytocompatibility of graphene for both fibroblast and neuron. Good cell-substrate interactions between neurons and G-C nanocomposites were found on samples with appropriate compositions. The results suggest this unique nanocomposite system may be a promising substrate material used for the fabrication of implantable neural electrodes.

Overall, these studies confirmed the bio-adhesive property of chitosan. More importantly, the developed chitosan-based materials also have great potential in the fields of neural tissue engineering and neuroprosthetics.

TABLE OF CONTENTS

Chapter Page

CHAPTER I 1
INTRODUCTION 1
1.1 Chitosan 1
1.1.1 Structure-Properties Relationship 1
1.1.1.1 Role of DDA 1
1.1.1.2 Role of MW 3
1.1.2 Biomedical Applications 3
1.2 Neural Engineering 4
1.2.1 Neural Tissue Engineering 7
1.2.2 Neuroprosthetics 10
1.3 Rationale and Objectives 14
CHAPTER II 17
CHITOSAN-AGAROSE HYDROGELS FOR BRAIN REPAIR 17
2.1 Introduction 17
2.2 Preliminary Study for Chitosan Selection 18
2.2.1 Rationales 18
2.2.2 Results & Conclusion 18
2.3 C-A Hydrogels for Brain Repair 20
2.3.1 Rationales 20
2.3.1.1 Sample preparation 20
2.3.1.2 Sample characterization 20
2.3.1.3 Primary cortical neuron culture 21
2.3.1.4 Fluorescent microscopy 21
2.3.1.5 Assessment of neuron responses to substrates 22
2.3.1.6 Statistical analysis 25
2.3.2 Experiments 25
2.3.2.1 Preparation of C-A 25
2.3.2.2 Rheological study of C-A 26
2.3.2.3 Morphological study of C-A 26
2.3.2.4 Primary cortical neuron culture on C-A 26
2.3.2.5 Neuron adhesion on C-A 27
2.3.2.6 Neurite extension on C-A 27
2.3.2.7 Neuron morphology on C-A 27
2.3.2.8 Statistics 27
2.3.3 Results & Discussion 28
2.3.3.1 Rheological study of C-A 28
2.3.3.2 Morphological study of C-A 28
2.3.3.3 Neuron adhesion on C-A 33
2.3.3.4 Neurite extension on C-A 36

2.3.3.5 Neuron morphology on C-A 38
2.4 Conclusions & Significance 43
CHAPTER III 44
GRAPHENE-CHITOSAN NANOCOMPOSITES FOR NEUROPROSTHETICS 44
3.1 Introduction 44
3.2 G-C Nanocomposites for Neuroprosthetics 46
3.2.1 Rationales 46
3.2.1.1 Sample preparation 46
3.2.1.2 Sample characterization 46
3.2.1.3 Biocompatibility of G 47
3.2.1.4 Neuron responses to substrates 47
3.2.2 Experiments 48
3.2.2.1 Preparation of G-C 48
3.2.2.2 Electrical property of G-C 48
3.2.2.3 Surface morphology and topography of G-C 48
3.2.2.4 Cytotoxicity of G 49
3.2.2.5 Neuron adhesion on G-C 50
3.2.2.6 Neuron morphology on G-C 50
3.2.2.7 Statistics 51
3.2.3 Results & Discussion 51
3.2.3.1 Preparation of G-C 51
3.2.3.2 Electrical property of G-C 54
3.2.3.3 Surface morphology and topography of G-C 54
3.2.3.4 Cytotoxicity of G 58
3.2.3.5 Neuronal responses to G-C 64
3.3 Conclusions 64
CHAPTER IV 65
GENERAL CONCLUSIONS AND FUTURE PERSPECTIVES 65
LIST OF REFERENCES 67
VITA 78

LIST OF TABLES

Table Page

Table 1.1 Main applications of chitosan as biomaterials 5
Table 1.2 Main properties of chitosan in biomedical applications 6
Table 2.1 Methods for assessment for neurite growth 24
Table 3.1 Formulations for G-C nanocomposites 49
Table 3.2 Electrical resistance of PG, G-C and silicon wafer 56

LIST OF FIGURES

Figure Page

Figure 1.1 Chemical structure of chitosan 2
Figure 1.2 Schematic of events following traumatic brain injury 8
Figure 1.3 Combination of tissue scaffold, cell transplantation and drug delivery 9
Figure 1.4 Principles, applications and challenge of implantable neural electrodes 11
Figure 1.5 Designs of multichannel recording electrode arrays 13
Figure 2.1 Neuron growth on C-A prepared with different types of chitosan 19
Figure 2.2 Principle of confocal microscopy 23
Figure 2.3 Equilibrium modulus G versus chitosan concentration 29
Figure 2.4 Photograph and light microscope images of hydrogels 30
Figure 2.5 SEM images showing structure of hydrogels 31-32
Figure 2.6 Schematic of phase separation of C-A as a result of neutralization 34
Figure 2.7 Cell densities versus chitosan concentration in C-A hydrogels 35
Figure 2.8 Percentages of neurons with different lengths of neurite versus C 37
Figure 2.9 Confocal images of the neuron network on C-A 39
Figure 2.10 Representative images showing neuron morphology on C-A 40
Figure 2.11 “Simulation” of neurite differentiations 41
Figure 3.1 Photograph of G-C dispersions 52
Figure 3.2 Chemical structure of chitosan and water soluble graphene 53
Figure 3.3 Photograph of free standing G-C films 55
Figure 3.4 SEM images showing the surface morphology of samples 57
Figure 3.5 AFM images showing the surface topography of samples 59
Figure 3.6 Cytotoxicity of graphene showing high survival rate of cells 60
Figure 3.7 Cell adhesion of N2a and cortical neuron 61
Figure 3.8 SEM images of primary cortical neuron growing on samples 63

CHAPTER I

INTRODUCTION

1.1 Chitosan

Chitosan is a naturally occurring linear polysaccharide derived from chitin by deacetylation of the N-acetyl-glucosamine residues under alkaline conditions or by enzymatic hydrolysis in the presence of a chitin deacetylase.[1] It is widely investigated for numerous applications in the life sciences, including cosmetics, dietetics, pharmacology, and biomaterials.[2] The chemical structure of chitosan largely determines its physical properties and applications. In this section, the structure-properties relationship of chitosan in solutions will be briefly introduced and discussed. Its applications in biomedical fields will then be elucidated.

1.1.1 Structure-Properties Relationship

Fig. 1.1 shows the chemical structure of chitosan. Because the temperatures of glass transition and melting of chitosan are higher than its temperature of thermal decomposition, the fabrication of chitosan is necessarily processed from solutions.[2] Therefore, the most important physical state for this polymer is solution. When studying solutions of chitosan, one of the key parameters need to be considered is the degree of deacetylation (DDA), which distinguishes chitosan from chitin. Molecular weight (MW) also plays critical roles for the properties of chitosan in solutions.

1.1.1.1 Role of DDA

When DDA is higher than 40%, the polymer is soluble in dilute acidic solutions and is defined as chitosan. This behavior is associated to the fact that the protonated amine groups of glucosamine residues in acidic solutions interrupt the intrachain hydrogen bonds and make solvent/polymer interactions more favorable.[2] The value of the intrinsic pK_a of chitosan is found to be close to 6.5 when DDA is higher than 75%. That is, chitosan with DDA value higher than 75% is soluble in a solution with a pH value lower than 6.5, ignoring the effects from MW. The relation between DDA and pK_a of chitosan is quite complicated and requires a good understanding of polymer science. Readers are encouraged to refer to the extensive work from Sorlier et al. for more details.[3] In this study, we are mainly concerned about the fact that a certain

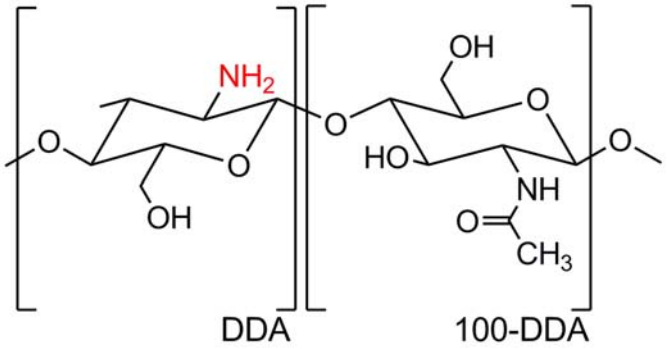

Figure 1.1 Chemical structure of chitosan.

amount of acid is required to solubilize chitosan in water, which is the most preferred solvent for biomedical applications.

1.1.1.2 Role of MW

Thermodynamics suggests a decreased solubility of neutral polymers with an increase of MW.[4] In the case of chitosan, the possibility of intrachain association by hydrogen bonding plays an additional role.[2] When MW increases, aggregation between polymer chains becomes favorable and the ionic strength becomes sufficiently high to favor the condensation of the counterions. In addition to the intrachain association, an increase in MW always results in an increase in viscosity of the solution. Therefore, it is often difficult to prepare chitosan solutions with a concentration above 2-3 wt%. Furthermore, decreasing the MW could potentially increase the concentration of the solution and improve the solubility of the polymer.

1.1.2 Biomedical Applications

Chitosan has been extensively studied as a biomaterial due to its excellent properties, such as biocompatibility and biodegradability. For biomedical applications, it can be fabricated into a variety of forms, including hydrogels, films, fibers, sponges, and micro- / nano-particles.[2]

Tissue scaffold is one of the most important applications of chitosan. By crosslinking chitosan with glycerophosphate, Chenite et al. successfully prepared thermally sensitive neutral chitosan solutions based on chitosan/polyol salts.[5] The solutions can gel at physiological temperature, and are able to deliver biologically active growth factors in vivo and serve as an encapsulating matrix for living chondrocytes for tissue engineering applications. Subsequent works using similar techniques have also been able to achieve a thermoresponsive system.[6-9] In the form of film, chitosan can be fabricated into conduit and used as a tissue scaffold.[10] Artificial poly(glycolic acid)-chitosan tube coated with recombinant L1-Fc promotes axonal regeneration and remyelination, and has been shown capable of guiding nerve regeneration.[11]

Drug/protein/gene delivery is an important domain where chitosan micro-/nano-particles are extensively employed. The positively charged chitosan chains can be easily complexed with negatively charged DNAs and proteins.[12] A simple precipitation process to prepare chitosan microparticles without using any organic solvent was developed by Berthold et al.[13] By simply

adding sodium sulfate (precipitant) into chitosan solution, the authors successfully prepared chitosan microparticles with size around 1 μm. The drug release behavior of the microparticles was tested in vitro using side-by-side diffusion cells and up to 30.5% loading was achieved with prednisolone sodium phosphate. The most widely used precipitant for the formation of chitosan nanoparticles is tripolyphosphate (TPP).[12, 14, 15] Typically, a size ranging from 100 nm to 250 nm is suitable for the delivery of gene or protein macromolecules. In order to fabricate chitosan nanoparticles with predetermined properties, variations in chitosan molecular weight, chitosan concentration, the weight ratio of chitosan to TPP, and solution pH value were examined systematically for their effects on the particle size, intensity of surface charge, and tendency of particle aggregation.[12] The authors also examined the particle morphology using transmission electron microscope (TEM) and confirmed a semicrystallization mechanism during the particle formation and growth, which could bear important implications on gene/protein encapsulation and release mechanisms.

Other biomedical applications of chitosan include surface modification, dialysis membrane, sutures, etc.[1] **Table 1.1** summarizes the main applications of chitosan in the field of biomaterials. **Table 1.2** lists the important properties of chitosan related to biomedical applications.

1.2 Neural Engineering

Neural engineering is a discipline that uses engineering techniques to understand, repair, replace, enhance, or treat the diseases of nervous systems. Due to its biological and engineering nature, many other disciplines are involved in its development, such as computational neuroscience, experimental neuroscience, clinical neurology, electrical engineering and signal processing, robotics, cybernetics, computer engineering, neural tissue engineering, materials science, and nanotechnology.[16] In the present study, we will mainly focus on the two major domains in neural engineering: neural tissue engineering and neuroprosthetics. For tissue engineering, our work specifically aims to address problems encountered in brain repair.

Traumatic brain injury (TBI) occurs when an external physical insult causes damages in the brain. Because the injury is an on-going process, the primary damage could lead to a cascade

Table 1.1 Main applications of chitosan as biomaterials.[1]

Form	Application	Route of delivery/properties
Beads	Drug delivery Enzyme immobilization	Oral
Micro-spheres		Oral, implantable, ocular, injectable
Coatings	Surface modification Textile finishes	Chitosan increases mucoadhesivity of alginate capsules
Fibers	Medical textiles Sutures	Biodegradable
Nano-fibers	Guided bone regeneration Scaffold for nerve tissue regeneration	
Films	Wound care Dialysis membrane	
Powder	Adsorbent for pharmaceutical and medical devices Surgical glove powder Enzyme immobilization	
Sponge	Mucosomal haemostatic dressing Wound dressing Drug delivery Enzyme entrapment	
Shaped objects	Orthopaedics Contact lenses	
Solutions	Cosmetics Bacteriostatic agent Haemostatic agent Anticoagulants Anti-tumour agent	Moisture holding Oral, nasal Complex formation – gene delivery
Gels	Delivery vehicle Implants, coatings Tissue engineering	
Tablets	Compressed diluent Disintegrating agent	Oral, buccal
Capsules	Delivery vehicle	

Table 1.2 Main properties of chitosan in biomedical applications.[1]

Properties		
Biodegradability	Antibacterial	Renewable
Biocompatibility	Immunoadjuvant	Absorption promotes
Bioadhesivity	Antithrombogenic	Non-toxicity
Polycationic substance	Film forming	Non-allergenic
Antifungal	Hydrating agent	Anticholesteremic agent

of deleterious events that can affect cell body and axonal function, resulting in continued dysfunction and prolonged degeneration. Therefore, patients often suffer not only from the immediate post-injury complications, but also the long-term problems associated with TBI, such as Parkinson's disease, Alzheimer's diseases, post-traumatic dementia, etc.[17] **Fig. 1.2** shows the events following TBI, involving a dynamic interplay between events promoting neural repair and regeneration, and those of damage and inhibition.[18] A better understanding of the mechanisms on both sides of the response can aid in the development of more effective clinical treatments for TBI. Each year, there are about 1.4 million people in the United States experience a TBI.[17] As one of the leading causes of death and disability, TBI poses a staggering financial burden to the society, with an estimated expense of over $56 billion per year for medical care. Therefore, it is urgent to develop clinically effective treatments to alleviate the pains of both patients and the society.

1.2.1 Neural Tissue Engineering

The main on-going researches for neuroprotection and neuroregeneration in injured central nervous system (CNS) include tissue scaffold, cell transplantation, and drug delivery.[19] **Fig. 1.3** shows a scheme of the combination of these three approaches applied in brain repair. An artificial tissue scaffold can be implanted into the damaged region in the brain tissue, serving as a structural support to the surrounding tissue to minimize secondary cellular degeneration. Both neural stem cells and drugs can be delivered by the scaffold. Patient's neurons from the adjacent parenchyma can also infiltrate the scaffold, which potentially promotes local tissue regeneration.

Because the scaffold is the platform for the delivery of cell and drug as well as neuron regeneration, its properties are critical to achieve all of these functions. The scaffold should provide a friendly environment for both resident neurons and implanted neurons by mimicking some of the features of the natural extracellular matrix (ECM) in the neural tissue. It should be neuron-adhesive to offer anchorage points that allow neuron adhesion and neurite outgrowth. It should be permissive, allowing cell migration and tissue remodeling as well as the diffusion of nutrients, metabolites, and soluble factors. The mechanical properties should match the brain tissue, because study has shown the mechanical properties of biomaterials are critical for neuron adhesion and neurite outgrowth.[20] Biodegradability is favored for brain repair since no foreign

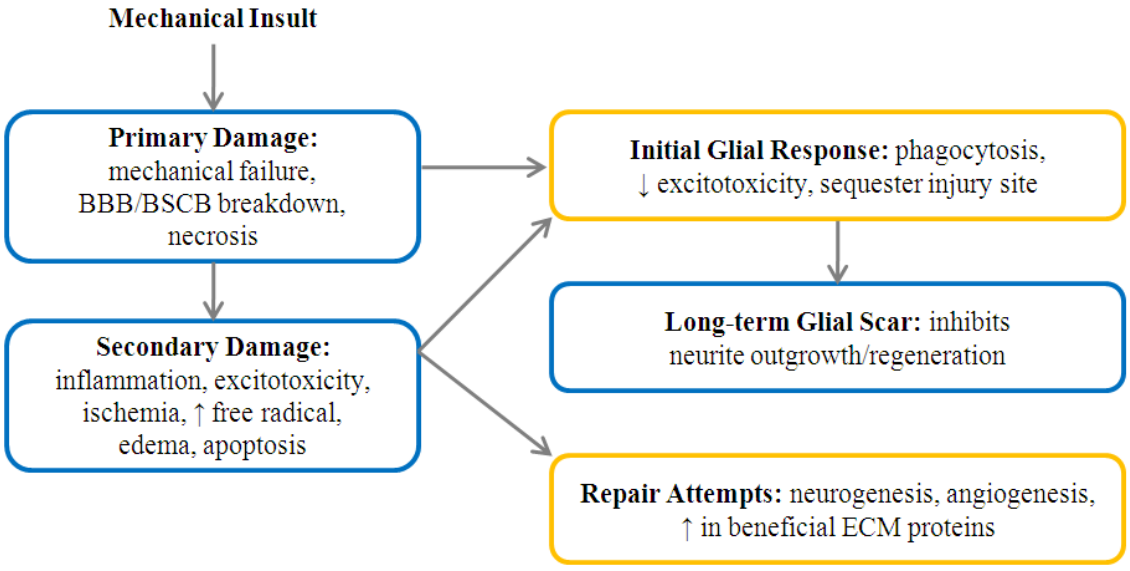

Figure 1.2 Schematic of events following traumatic brain injury (TBI): (blue boxes) damage and inhibition of regeneration; (orange boxes) permissive and reparative mechanisms. A better understanding of the mechanisms on both sides of the response can aid in the development of more effective clinical treatments for traumatic injury to the CNS.[18]

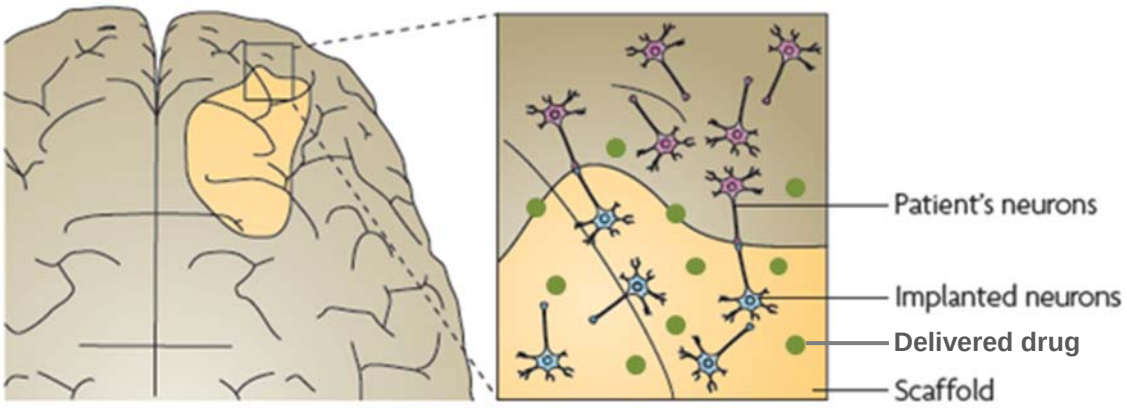

Figure 1.3 Combination of tissue scaffold, cell transplantation and drug delivery for the repair of damaged brain tissue. Adapted from reference *Nature Review Neuroscience* 10 (2009) 682-692.[19]

substance will remain in the injury site once new tissues have formed in place. When being used for drug delivery, the chemical and structural properties of the scaffold also need to be optimized.

Hydrogels have been favored as tissue scaffold materials for their excellent properties. The porous structure allows for infiltration of cells as well as the diffusion of drugs, gases, nutrients, and waste products. The mechanical properties of hydrogels can be tuned by changing the density of the crosslinking points, allowing low interfacial tensions between the scaffold and human tissue. Furthermore, most hydrogels are degradable by enzymes present in the human body, a desirable feature for brain repair.

Currently, hydrogels based on both natural (e.g., agarose, alginate, hyaluronan, etc.) and synthetic (e.g., polyethylene glycol, poly(2-hydroxyethyl methacrylate), etc.) polymers are being studied for neural engineering.[21] One of the great limitations of these hydrogels is the need for chemically incorporation of neuron-adhesive protein or peptide sequences due to their intrinsic non-adhesive nature.[22-24] Potential problems associated with chemical functionalization include: (1) complex, costly and time-consuming process and (2) introduction of toxic organic solvents during preparation that could be harmful for cellular growth. *A simply prepared neuron-adhesive hydrogel system without any chemical reaction would have great potential for neural tissue engineering.*

1.2.2 Neuroprosthetics

Unlike neural tissue engineering, which aims to protect and repair the injured tissue right after the injury, neuroprosthetics are more like a "make-up" approach for a damaged nervous system. It generally involves artificial devices to replace the function of impaired nervous systems or sensory organs, such as restoring sights, hearing, movement, ability to communicate, and even cognitive functions. The most widely used neuroprosthetic device is the cochlear implant, which has been benefiting approximately 100,000 people worldwide as of 2006.[25]

Nowadays, chronically implanted neural electrodes recording signals from individual neurons in human brain rekindle the hope of numerous patients suffering from full or partial paralysis.[26-28] **Fig. 1.4** is a scheme showing the principle and potential applications of this kind of device as well as the greatest challenges it faces currently. The neural electrodes, which can be in

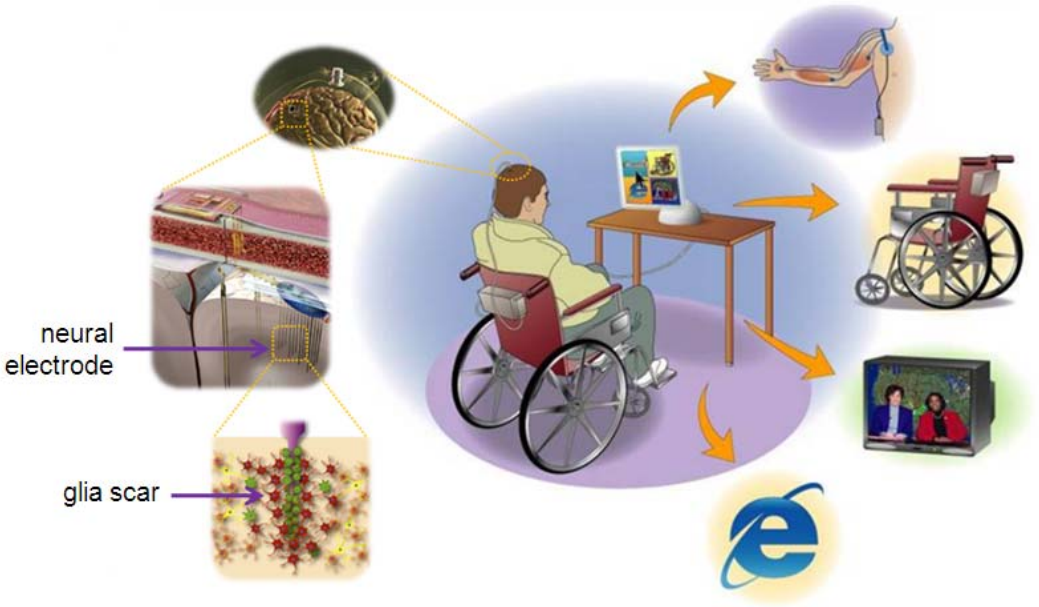

Figure 1.4 Principles, applications and challenge of implantable neural electrodes.

the form of metal wires or silicon and/or polymer shanks, are inserted into the brain cortex. If functioning properly, the device can record the action potentials from the adjacent healthy neurons. The collected signals are then transported to an external device, which typically is a computer. The signals are processed, analyzed, and translated into commands. Then the commands are utilized for controlling prosthetic devices, such as artificial arms, wheelchairs, entertainment media, etc.

To date, several different multichannel recording electrode arrays have been designed (**Fig. 1.5**).[29-32] Most of them are fabricated from silicon taking advantage of the well-established manufacturing process used in the semiconductor industry. Although the present implant systems are well studied and perform as intended in short-term investigations, the greatest challenge of the implants for clinical applications is its unreliable long-term performance.[33] For instance, a 40% drop in the number of functional electrodes between 1 and 18 months was reported in the study of Nicolelis et al.[29] Similar observations have also been reported by other researchers.[31, 34]

Scientific studies suggest that the long-term performance problem is likely due to the tissue response that the brain mounts against implanted electrodes.[33] Several factors could potentially contribute to the tissue response: (1) the mechanical trauma of insertion severing capillaries, extracellular matrix, glial and neuronal cell processes; (2) the long-term inflammation induced by the presence of the insoluble device; (3) the biocompatibility of the implanted substrate material; and (4) the chronic micromotion-induced mechanical strains around the implant interface. Eventually, the response results in the formation of an encapsulating glial scar (**Fig. 1.4**) and a poor integration between the device and neural tissue.

Current approaches to minimize this tissue response include: (1) advanced neural probe design, (2) surface modification of the existing implanted substrate, and (3) drug delivery locally or systemically to therapeutically influence the cellular responses.[33] A recent study from Dr. Kipke's group at the University of Michigan reported the fabrication of a parylene-based probe with a thick shank and an integrated thin lateral platform with recording site.[35] Biological studies showed a reduced tissue encapsulation and higher neuronal density around the recording site compared with the thick shank. It is suggested that the electrode performance can be maintained in long-term by attracting and preserving neurons near the recording sites. A variety of materials

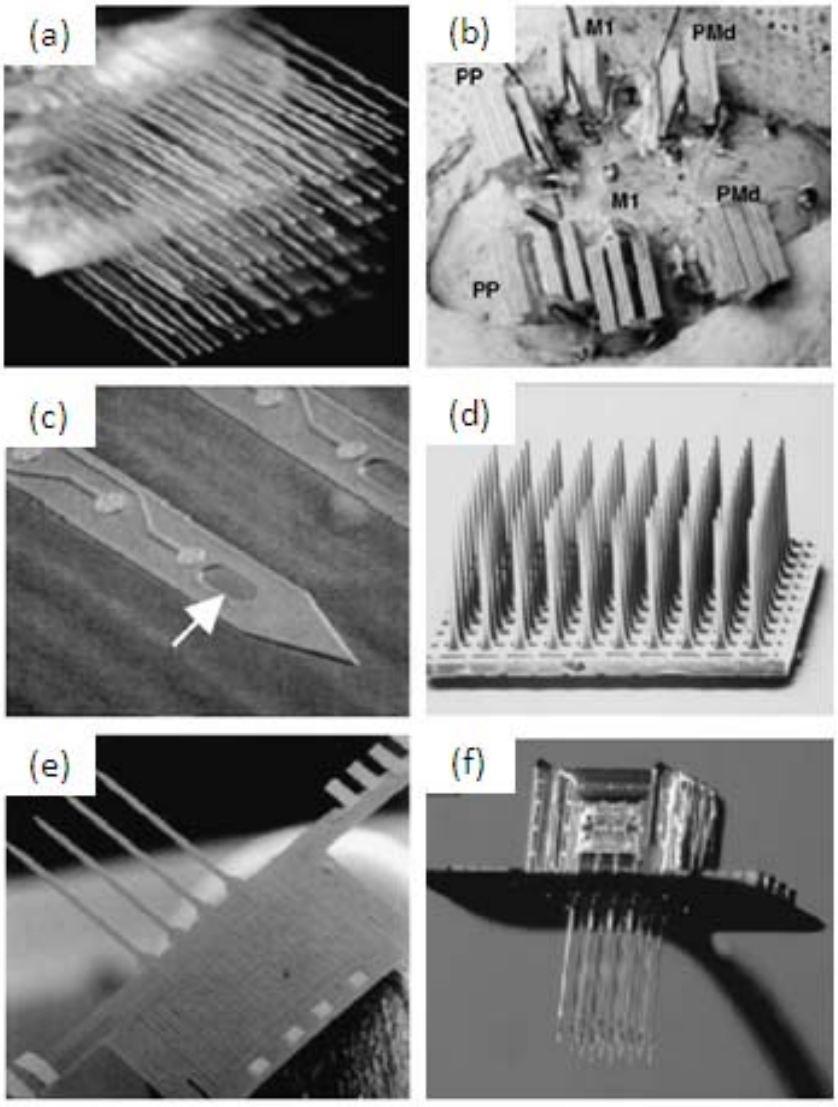

Figure 1.5 Designs of multichannel recording electrode arrays: (a-b) wire electrode arrays;[29] (c) a single electrode shank with multiple electrode sites;[30] (d) Utah Electrode Array formed from a single block of silicon;[31] (e-f) multiple planar arrays of Michigan Electrodes are stacked together to create a three-dimensional array.[32]

have been used to modify the substrate surface, such as cell adhesion small polypeptides/proteins (e.g., poly-L-lysine and laminin[36]) and oligopeptides (e.g., Arg-Gly-Asp (RGD) and Tyr-Ile-Gly-Ser-Arg (YIGSR)[37]). Conductive polymer coatings, including polypyrrole and poly(3,4-ethylenedioxythiophene), have also been studied for their ability to overcome the encapsulation barrier and improve electrical characteristics by increasing electrode sensitivity.[38-41] Drug release is another option that could potentially promote neuronal survival and growth. On the one hand, growth factors and chemoattractants can be used to attract neuron migration towards the electrodes and facilitate neuron regeneration.[42] On the other hand, immunosuppressant molecules such as Dexamethasone[43] and Cyclosporin-A[44] can be used to reduce the initial immune response and potentially the glial scar formation. Other drugs like minocycline[45-47] also show their capability to protect neurons against excitotoxicity by inhibiting activation and proliferation of microglia. Although moderate success has been achieved by some of the methods in reducing the tissue response, devices with long-term reliable performance are still not clinically applicable.

Simply modifying the surface of existing substrate materials will not be able to eliminate the micromotion induced by the mechanical mismatch between the tissue and electrodes, which is believed to profoundly contribute to the chronic immune response.[33] Recently, the neural interface community is focusing on exploring brand new implantable materials that can be used for neural electrodes with reliable chronic performance.[48] The new materials should be flexible with low interfacial tension with human brain and ability to change its shape along with tissue deformation. Electrical conductivity is required for the normal function of neural recording electrodes. The substrate should be neuro-adhesive to ensure good neuron-substrate interactions. In addition, good biocompatibility and biostability are always required for implantable biomaterials intended for chronic use. *Developing substrate materials meeting all of these criteria is still a major challenge in the field of neuroprosthetics.*

1.3 Rationale and Objectives

Chitosan has been studied for nerve tissue regeneration. Until now, most of the works are focusing on its film and scaffold forms for nerve regeneration in the peripheral nervous system and spinal cord.[6, 10, 49] *The present study, from another aspect, aims to take advantage of the bio-*

adhesive property of chitosan and investigate its potential applications in neural engineering, specifically in the fields of brain repair and neuroprosthetics (brain-computer interface).

One of the main issues in neural engineering is the poor ability of neuronal cells to attach and grow on most biomaterials. A variety of strategies have been developed to stimulate neuron adhesion and growth.[50] Scientific studies have shown that chemical factors (e.g., ECM proteins and certain peptide sequences[51, 52]), topographical features of biomaterials,[53-55] and substrate stiffness play critical roles in neuron adhesion, growth, and tissue remodeling. Previous studies have shown the ability of chitosan to facilitate attachment of dorsal root ganglion (DRG),[10, 56] keratinocytes,[57] fibroblasts,[57] and Schwann cells,[58] indicating a nonspecific interaction between cells and chitosan. Such characteristic could be attributed to the electrostatic attractive force between the positive charges of the protonated amine groups along chitosan chains and the negative charges of the phospholipid structure of the cell membrane. *We propose that this bio-adhesive property of chitosan could potentially improve neuron adhesion and neurite outgrowth, making chitosan a promising biomaterial candidate in the field of neural engineering.*

In Chapter II, *we simply blended chitosan with a well-studied hydrogel system (agarose).* This hydrogel system showed good neuron-adhesive property. The concentration of chitosan also had great influence on neurite extension. A "steric hindrance" hypothesis was proposed to explain the observations in biological study. It implies that a proper adjustment of the blend composition could directly impact the morphological development of neurons, and could be used as a simple yet versatile approach to obtain desirable neuronal structures. The simplicity of preparing this hydrogel system also allows for future applications of agarose-based hydrogels for neural tissue repair.

In Chapter III, *we developed a brand new graphene-chitosan nanocomposite system as a potential substrate material for implantable neural electrodes.* The free standing film prepared by air evaporation showed good flexibility. The electrical conductivity of graphene was maintained after the incorporation of chitosan. Biological studies showed good biocompatibility of graphene and good cell-substrate interaction between neuron and G-C nanocomposites with proper compositions. The promising results indicated the potential impact of G-C nanocomposites on the clinical translation of neural interface technology by improving the long-

lasting performance of the implant through fundamental changes of the substrate material used for implant fabrication.

CHAPTER II

CHITOSAN-AGAROSE HYDROGELS FOR BRAIN REPAIR

An article presenting part of the results in this chapter has been published on Biomacromolecules [Zheng Cao, Ryan Gilbert, Wei He. Simple agarose-chitosan gel composite system for enhanced neuronal growth in three dimensions. *Biomacromolecules* **2009**, 10 (10), 2954-2959]. Published data include: Fig. 2.3, Fig. 2.4, Fig. 2.5 (a, d and g), Fig. 2.6, Fig. 2.7, Fig. 2.8, Fig. 2.9, Fig. 2.10, and Fig. 2.11. Section 2.3.2, 2.3.3 and 2.4 are directly cited from the article with a few modifications. Section 2.1, 2.2 and 2.3.1 are newly written.

The first author (Zheng Cao) finished all of the experiments in this study. The third and corresponding author (Dr. Wei He) is advisor of Zheng Cao and financially supported this work. The second author (Dr. Ryan Gilbert) is a collaborator of Dr. Wei He, and gave professional advice on this work.

2.1 Introduction

Chitosan itself can be fabricated into a three-dimensional (3D) hydrogel using salts or other agents. However, our preliminary data indicate that chitosan hydrogel is non-permissive for neural growth. A well studied hydrogel system, agarose, was selected as the hydrogel matrix for this study. Agarose, a biocompatible polysaccharide, is widely investigated as a 3D scaffold for neural engineering. In the form of a hydrogel, agarose has porous structure[59] and provides a friendly environment for cellular spreading and proliferation.[60, 61] The main issue for agarose to be used as a neural scaffold is its incapability to support cell attachment.[62] Previous study has shown chemical functionalization of agarose with neuro-adhesive components could improve E9 chick DRG neurite extension, but the complex chemical process is costly and time-consuming.[60] Here, we chose to blend chitosan into agarose hydrogel to simplify the preparation process and investigate its potential application for brain repair. The influences of chitosan on neuron adhesion and neurite extension were also studied.

2.2 Preliminary Study for Chitosan Selection

2.2.1 Rationales

As mentioned earlier, the values of DDA and MW could affect the physical properties of chitosan. Currently, there are a variety of chitosan products available in the market, with different origins and chemical structures. Because it is not practical to perform the work using all types of chitosan, we need to indentify one most suited for the intended applications first. To avoid the influences from origin and processing, a series of chitosan from one vendor will be compared. Because characterization and modification of chitosan are not parts of this study, only products with known values of DDA and MW were considered. After a brief investigation, a series of chitosan (Sigma) with similar values of DDA (75% - 85%) but different MW (LMW: 50,000-190,000 g/mol; MMW: 190,000-310,000 g/mol; HMW: 310,000-375,000 g/mol) were selected for preliminary study. Because chitosan with the same MW but different DDA are not readily available, the effect of DDA on neuron growth will not be considered here.

The three types of chitosan were generously provided by Dr. Kevin M. Kit (Department of Materials Science & Engineering, UTK) and Dr. Svetlana Zivanovic (Department of Food Science and Technology, UTK). Three chitosan-agarose (C-A) hydrogels with consistent concentration (both C and A: 1 wt%) were prepared. Plain agarose hydrogels (1 wt%) served as a control. Primary chick cortical neurons were cultured on the samples for 3 days and characterized using confocal microscopy. Hydrogel sample supporting the most neuron adhesion (i.e., highest cell density) and neurite outgrowth (i.e., best neural network) is considered as the premium substrate, and chitosan used for that sample will be employed for the rest of the study. Detailed procedures related to sample preparation and in vitro study are described in the following sections.

2.2.2 Results & Conclusion

A drastic increase of cell number was observed on all C-A hydrogels (**Fig. 2.1 (a) – (c)**) compared with plain agarose hydrogel (**Fig. 2.1 (d)**), which confirms our hypothesis that chitosan could improve neuron adhesion. In addition, a better neural network was developed on

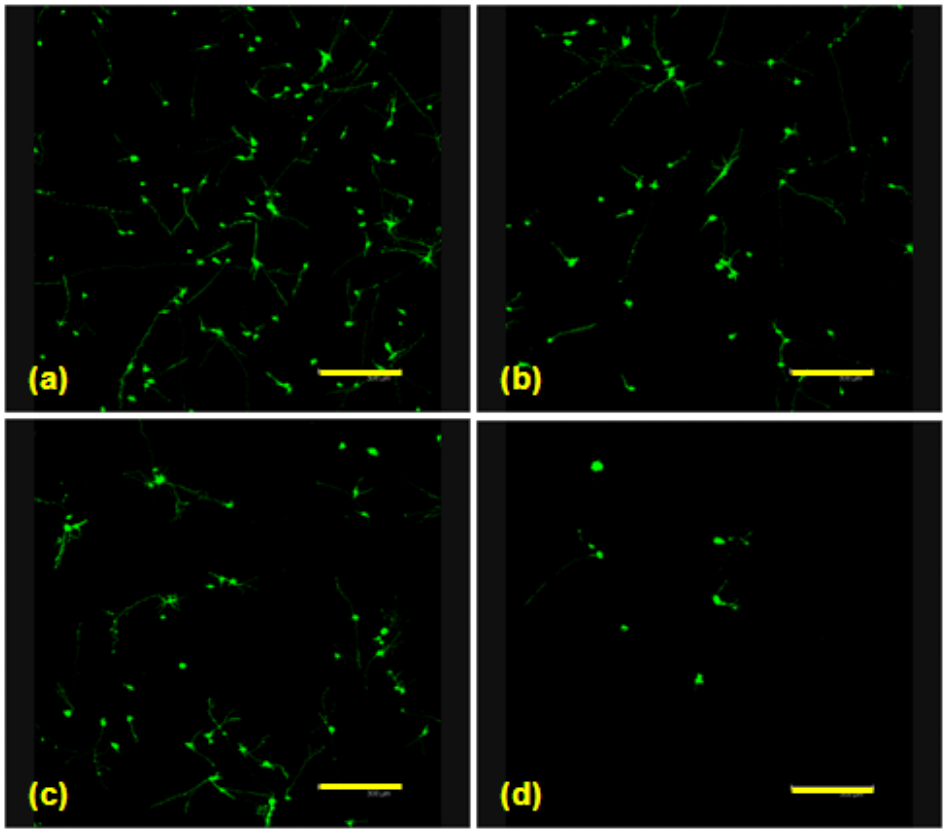

Figure 2.1 Neuron growth on C-A prepared with different types of chitosan: (a) LMW, (b) MMW, (c) HMW, and (d) plain agarose. Scale bar = 300 μm.

C-A hydrogel made from LMW chitosan (**Fig. 2.1 (a)**). Therefore, LMW chitosan was selected for the rest of the study.

2.3 C-A Hydrogels for Brain Repair

2.3.1 Rationales

This section briefly introduces the rationales behind the experimental design and special techniques used in this chapter. Please see *section 2.3.2 Experiments* for detailed experiments.

2.3.1.1 Sample preparation

The concentration of chitosan is the only variable in sample preparation. As mentioned earlier, solutions with chitosan concentration above 3 wt% are not feasible due to the large increase in viscosity of the solution and the limited solubility of chitosan.[2] Therefore, the concentration of chitosan was kept below 3 wt%. Acetic acid aqueous solution was used to dissolve chitosan. SeaPrep® agarose was selected according to a previous study[60], and was kindly donated by Lonza Rockland. A consistent agarose concentration (1 wt%) was maintained for all the samples as this concentration of SeaPrep® agarose gel supported the best neurite outgrowth from chick DRG. Moderate heating (~60 °C) is required to dissolve this SeaPrep® agarose in water, and relatively low temperature (10 – 17 °C) is necessary for the solution to form a gel. Therefore, after plating final solutions in glass-bottom petri dishes, samples were kept in a refrigerator for gelation. Generally, all of the hydrogel compositions can gel within 20 min at 4 °C. A rinse with basic phosphate buffered saline (PBS) was applied for all C-A hydrogels to neutralize the acid. For biological study, samples also need to be sterilized. A 20 min UV exposure was utilized for sterilization as opposed to commonly used autoclave approach, considering the hydrating nature of the gel.

2.3.1.2 Sample characterization

Because studies have shown the mechanical properties of a substrate have great influence on neuron adhesion and growth,[20] the stiffness of the hydrogels was evaluated by a rheometer according to a previous study.[63] The purpose of this measurement is to determine if the incorporation of chitosan influences the mechanical properties of agarose gel, thereby affecting the neuron adhesion and growth on C-A hydrogels.

C-A hydrogels were as clear as plain agarose after gelation, but they turned into opaque after the basic rinse. Therefore, the structure of the hydrogels was characterized by light microscopy and scanning electron microscopy (SEM). The internal structure of the hydrogels was observed under a light microscope with oil lens for high magnification imaging. The surface structure of the samples was characterized by SEM.

2.3.1.3 Primary cortical neuron culture

Instead of using neuron cell lines, primary chick cortical neuron was used for the in vitro study to better represent the neuronal responses in real brain tissue. According to our previous experience, primary cortical neurons are especially "picky" and can only attach on specially treated substrates (e.g., laminin coated petri dish). Failure in adhesion will eventually lead to cell death. Cortical neurons were harvested from the forebrain of a 9-day old chick embryo. To disaggregate the forebrain tissue, a combination of chemical and mechanical dissociation methods was utilized to prepare a suspension of single cells. Cell purification can be achieved by incubating the cell suspension on a collagen coating. This process has been reported to provide culture with 97% of neuron composition.[64] It is worth noting that primary cortical neurons do not proliferate, which is different from commonly used neuron cell lines. Therefore, the number of neurons on substrates can only decrease due to cell death, but will not increase during culture.

2.3.1.4 Fluorescent microscopy

Because the neutralized C-A hydrogels were opaque, the cell cultures on these samples could not be directly observed under a inverted light microscope. Accordingly, a live staining technique (Live/Dead Viability/Cytotoxicity Kit for mammalian cells, Invitrogen) was applied to enable cell emitting green fluorescence under a fluorescent microscope. The principle behind this method is that live cells can absorb the nonfluorescent staining agent (calcein AM) and enzymatically convert it into fluorescent calcein, while dead cells are unable to achieve the conversion. In this way, only cells survived during the culture will be detected under the fluorescent microscope. To save time, images at certain magnifications were taken for all cultures first and analyzed later.

Because agarose gel is a 3D permissive scaffold for cell growth, a laser scanning confocal fluorescent microscope was used to collect signals throughout the hydrogel. Confocal

microscopy offers several advantages over a conventional optical microscopy, including the ability to control depth of field, elimination or reduction of background information away from the focal plane, and the capability to collect serial optical sections from thick specimens.[65] **Fig. 2.2** shows the principle of this technique. Using the software provided by the vendor, one composite image showing all the information from the serial sections is achievable. The signal can also be presented in different colors to show the 3D profile of the culture.

2.3.1.5 Assessment of neuron responses to substrates

There are a number of ways for assessing cellular responses to substrates. Cell viability is the most commonly used one. By counting cell number on the substrate after a certain period of culture and comparing with a positive or negative control, the biocompatibility of the substrate can be evaluated. Plain agarose hydrogel was used as a control for this study because we would like to see if the incorporation of chitosan could improve the neuron-adhesive property of agarose hydrogel. To obtain quantitative results, the cell number within a defined area of a substrate is counted and used to calculate the cell density (cells/cm^2).

How well can neurons differentiate on/within a substrate is another important criterion for neuron related study. For example, as shown in **Fig. 1.3**, the ultimate goal for neural tissue engineering is to build a good network among neuronal cells and realize their normal functions (signal transportation). The methods for assessing neurite outgrowth are well summarized by Radio and Mundy,[66] including semi-quantitative, quantitative, and biochemical assessments. Each of these categories has their advantages and disadvantages (**Table 2.1**). For semi-quantitative methods, the exact length of neurite will not be measured. It is only used for classifying cells into different groups, such as cells with neurites and cells without neurites. Therefore, the assessment can be simple and rapid, and no special technique or software is required. The results might be subjective, however, with a risk of scoring bias. Quantitative assessment, on the other hand, can be quite time-consuming and work-demanding if analysis is done by hands. Software could be employed for analysis, but it can be fairly expensive. Accuracy is the advantage of this kind of method. Neurite outgrowth can also be quantified using a variety of biochemical markers, based on the assumption that biomarkers correlate with both differentiation and increases in neurite length. Procedures, such as enzyme-linked

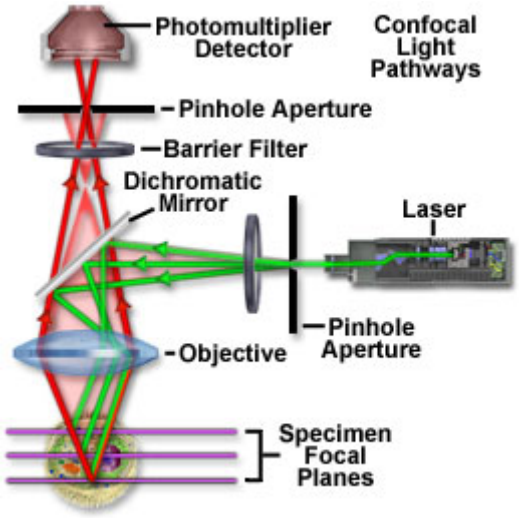

Figure 2.2 Principle of confocal microscopy.[65]

Table 2.1 Methods for assessment for neurite growth.

Method	Advantages	Disadvantages	Examples
Semi-quantitative	Rapid Simple Inexpensive	Can be subjective	Number of cell exhibiting neurites Percentage of cells exhibiting neurites Number of neurites per cell
Quantitative	Accurate	Time-consuming Greater amount of work Expensive	Length of the longest neurite Total neurite length Average neurite length
Biochemical	Rapid	Costly There may not be a direct relationship between the biomarker expression and neurite length.	ELISA Immunoblotting Proteomic techniques

immunosorbent assay (ELISA), immunoblotting, and proteomic techniques, are useful in high throughput screening. The measurement can be rapid, but the biochemical reagents used for marking neurites are often expensive. There is also a concern about the accuracy between the biomarker expression and the actual neurite length. Considering the availability of techniques and the cost of the assessments, a semi-quantitative method was selected for this study. Instead of just calculating the percentage of cells exhibiting neurites, we categorize cells into four groups according to the length of their longest neurite. Briefly, four different ranges of neurite length were predetermined, including 0 – 25 μm, 25 – 50 μm, 50 – 150 μm and >150 μm. Each cell on the substrate was classified into one of the four groups according to the length of its longest neurite. For example, if a neuron has four neurites and the longest one is 100 μm in length, this cell will be put into the 50 – 150 μm group. After all cells on one substrate were grouped, the percentage of cells exhibiting different length of neurites was calculated and compared.

2.3.1.6 Statistical analysis

Statistical analysis is a very important technique in biological studies. Considering the randomness and unpredictable variability during sample preparation and data collection, repetition must be conducted before achieving any solid conclusion. In this study, all cultures were repeated three times, meaning that each sample was subjected to cultures on three separate days. A statistical software (SAS) was used for the data analysis.

2.3.2 Experiments

2.3.2.1 Preparation of C-A

A series of C-A hydrogels with chitosan content varying between 0 and 3 wt% were prepared following a simple procedure. Hydrogels with higher chitosan concentration beyond 3 wt% are not feasible and reliable for cell culture work due to the large increase in the viscosity of the solution and the limited solubility of chitosan.[2] Briefly, chitosan (LMW, Sigma) was first dissolved in a 2.5 wt% acetic acid solution. SeaPrep® agarose (Lonza) (1 wt%) was then added to the chitosan solution and dissolved by heating the mixture in a 60 °C water bath. To prepare hydrogels for cell culture, 100 μl of the final solution was plated in a glass bottom petri dish (well: 1.4 cm in diameter, MatTek), and stored in a 4 °C refrigerator overnight to ensure

complete gelation. Neutralization was achieved by extensive rinsing of the hydrogel with basic phosphate buffered saline (PBS) solution (pH = 8.5). Plain agarose hydrogels (1 wt%) were prepared as a control following a similar procedure, without the addition of acetic acid and neutralization. All hydrogels were sterilized in sterile PBS solution (pH = 7.4) by UV light exposure for 20 min before the cell culture.

2.3.2.2 Rheological study of C-A

The mechanical stiffness of the hydrogel was determined by dynamic mechanical spectrometer (TA Instruments AR2000 rheometer, USA) at 37 °C with parallel plates. The complex modulus, G*, was determined at a constant strain (0.1%) for a frequency range of 0.1 to 100 rad/s. The stable plateau modulus, at frequencies between 0.1 and 10 rad/s, was used to approximate the equilibrium modulus, G, according to a previous study.[63]

2.3.2.3 Morphological study of C-A

The morphological structure of the hydrogels before and after basic buffer rinsing was directly imaged using a light microscope (Nikon Eclipse Ti, Japan) at a magnification of 100X. Then the samples were freeze-dried, sputter-coated with gold and imaged using a SEM (LEO 1525, Germany).

2.3.2.4 Primary cortical neuron culture on C-A

Cortical neurons were obtained from 9-day old chicken embryos. Forebrains of the embryo were dissected, minced into small pieces, and enzymatically dissociated with 0.25% trypsin in PBS for 20 min at 37 °C, followed by inactivation with medium containing 10% fetal bovine serum (FBS, Invitrogen). A cell pellet was obtained after a brief centrifugation, and mechanical trituration using a fire-polished Pasteur pipette was applied to further dissociate the cells. Cells were then preplated on a collagen-coated petri dish and incubated for 1 h at 37 °C in a 5% CO_2 atmosphere. Purified neuronal cells were collected and re-suspended for cell culture.

After counting, cells were seeded on sterile hydrogels with a density of 2×10^4 cells/cm^2, and cultured in Dulbecco's modified Eagle's medium supplemented with 10% FBS, 1% penicillin/streptomycin and 1% L-glutamine at 37 °C in a 5% CO_2 atmosphere for a predetermined time as specified in the following section. Nerve growth factor (NGF) is not

required to induce chick cortical neuron differentiation and neurite outgrowth.[67] Therefore, NGF was not used in the cortical cell culture. Each of the hydrogel compositions was tested three times, meaning that each hydrogel was subjected to cultures on three separate days.

2.3.2.5 Neuron adhesion on C-A

At the end of 3-day culture, cells were live stained with 0.05 v/v Calcein AM (Invitrogen) solution in PBS, and incubated at 37 °C in a 5% CO_2 atmosphere for 30 min. Samples were rinsed twice with PBS before and after fluorescence staining. Fluorescent images were taken using a 10X objective lens on a confocal microscope (Leica SP2, Germany). Neuron adhesion on the hydrogels was assessed by counting cell density (cells/cm^2).

2.3.2.6 Neurite extension on C-A

For neurite extension quantification, a cellular process being equal to or greater than 25 μm is defined as a neurite. The length of the longest neurite per neuron was used to analyze the percentage of neurons with different neurite outgrowth (25 – 50 μm, 50 – 150 μm, and >150 μm) on three representative areas for each 3-day cell culture sample.

2.3.2.7 Neuron morphology on C-A

Neuron morphology was analyzed for 5-day cell cultures following the same live staining procedure as describe above. The samples were imaged on the confocal microscope. The network of neurons was imaged at with a 10X lens, and detailed morphological images of representative cells were captured with a higher power lens (63X). In order to correlate the observed neuron morphology with the structure of various C-A hydrogels, surface features of the gels obtained from the light microscopy images were simulated by distributing different percentages of random dots (1 unit, representing the chitosan component) in a blank area (100 x 100 units, representing the agarose matrix) using a Matlab program.

2.3.2.8 Statistics

Data were analyzed using analysis of variance (ANOVA, SAS 2008), and least squares means were compared by Tukey's test. Differences were accepted at a significant difference value of $p < 0.05$. All data were reported as the mean ± standard deviation.

2.3.3 Results & Discussion

2.3.3.1 Rheological study of C-A

Recent work has demonstrated that the stiffness of substrates influenced the adhesion and morphology of tissue cells,[68, 69] and softer substrates were more favorable at facilitating neuronal differentiation than harder ones.[20] As one of the key features of agarose gel for nerve repair lies in its close mechanical matching with the neural tissue, it is important that such feature is not compromised with the blend of chitosan. Although the introduction of chitosan slightly decreased the value of G (plain agarose hydrogel: ~75 Pa; C-A hydrogels: 20 ~ 70 Pa), the stiffness of the C-A hydrogels were still on the order of 100 Pa (**Fig. 2.3**), which is very close to the stiffness of the brain tissue.[70] Therefore, from the mechanical property perspective, all of the C-A hydrogels are comparable to plain agarose and should have similar influence on neuronal growth.

The cause of slight reduction in the stiffness of the 0.33% C-A hydrogel is unclear. Clark et al.[71] have reported similar observation in the agar/gelatin co-gels, where the shear modulus of the gel first falls as gelatin is added and then increases again with more addition of gelatin. The authors attributed the minima to the interference effect, i.e., the concentrating action of the gelatin aggregation is insufficient to increase the gel strength of the initially formed agar phase to match the value of a pure agar gel until the gelatin concentration reaches beyond the phase inversion point. We speculate the chitosan molecule has similar interference effect on agarose in our hydrogel system, but the exact mechanism is beyond the scope of this study.

2.3.3.2 Morphological study of C-A

All non-rinsed C-A hydrogels were as clear as the plain agarose gel (not shown), but they displayed an opaque appearance after neutralization (**Fig. 2.4 (a)**). The extent of the opacity directly corresponds to increasing concentrations of chitosan. Light microscope images show aggregates within the agarose matrix (**Fig. 2.4 (b)**). A correlation between the density of aggregates and concentration of chitosan was observed too. The morphology of samples was also investigated using SEM. C-A hydrogel with 3.0 wt% of chitosan collapsed during sample preparation, thus images are not available for this composition. As shown in **Fig. 2.5**, plain agarose hydrogel and non-rinsed C-A hydrogels display opened porous structure, while rinsed C-

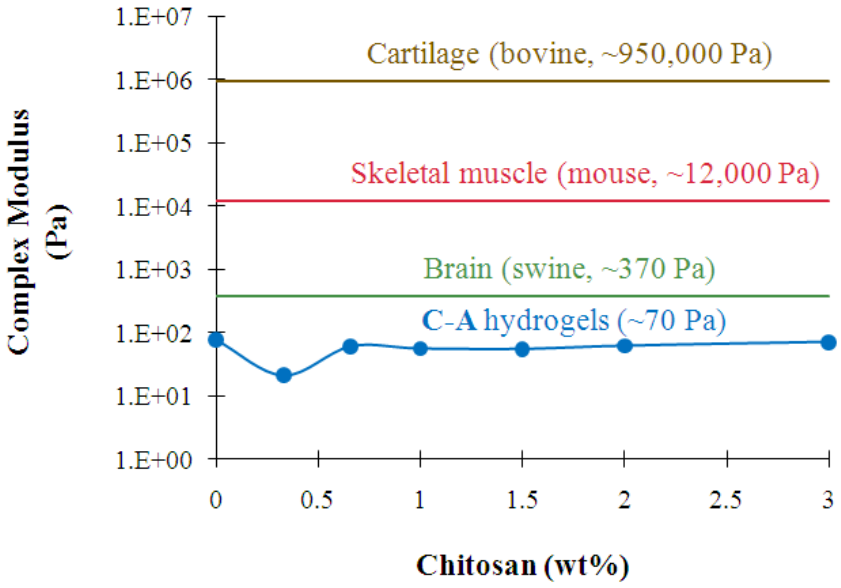

Figure 2.3 Equilibrium modulus G versus chitosan concentration: The stiffness of brain, skeletal muscle, and cartilage are presented for comparison.[70]

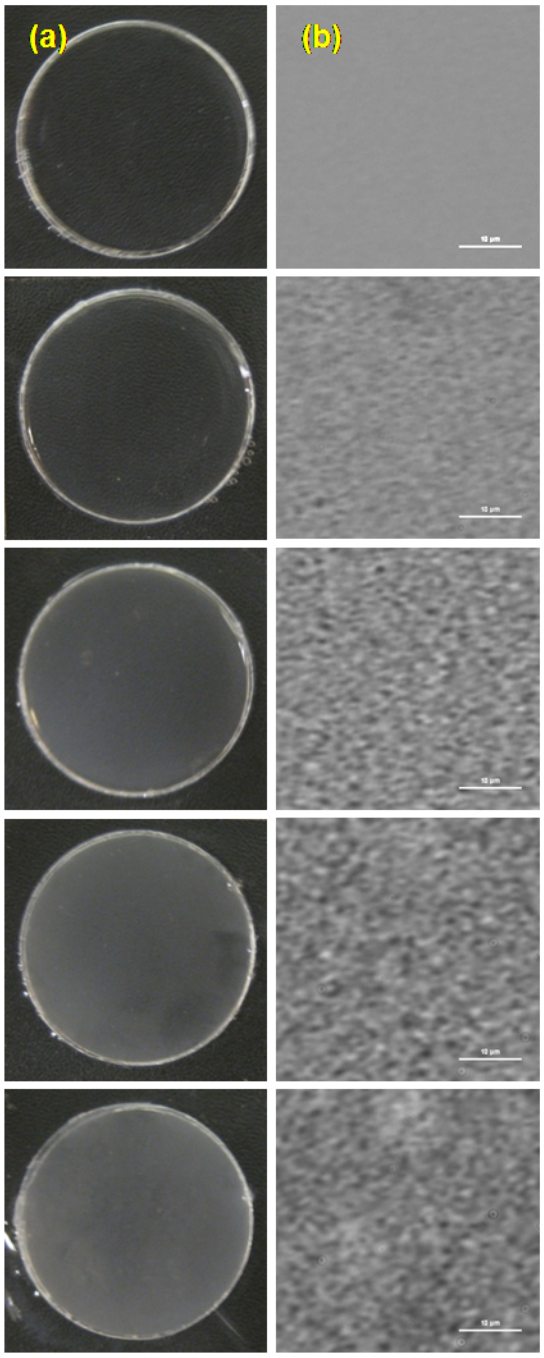

Figure 2.4 Photograph and light microscope images of hydrogels: (a) Photographs demonstrating the opaque appearance of C-A hydrogels compared with plain agarose gel and (b) light microscope images (100X) showing the structure of hydrogels. Concentration of chitosan from top to bottom: 0% (plain agarose), 0.33%, 1.0%, 2.0%, and 3.0%. Scale bar = 10 μm.

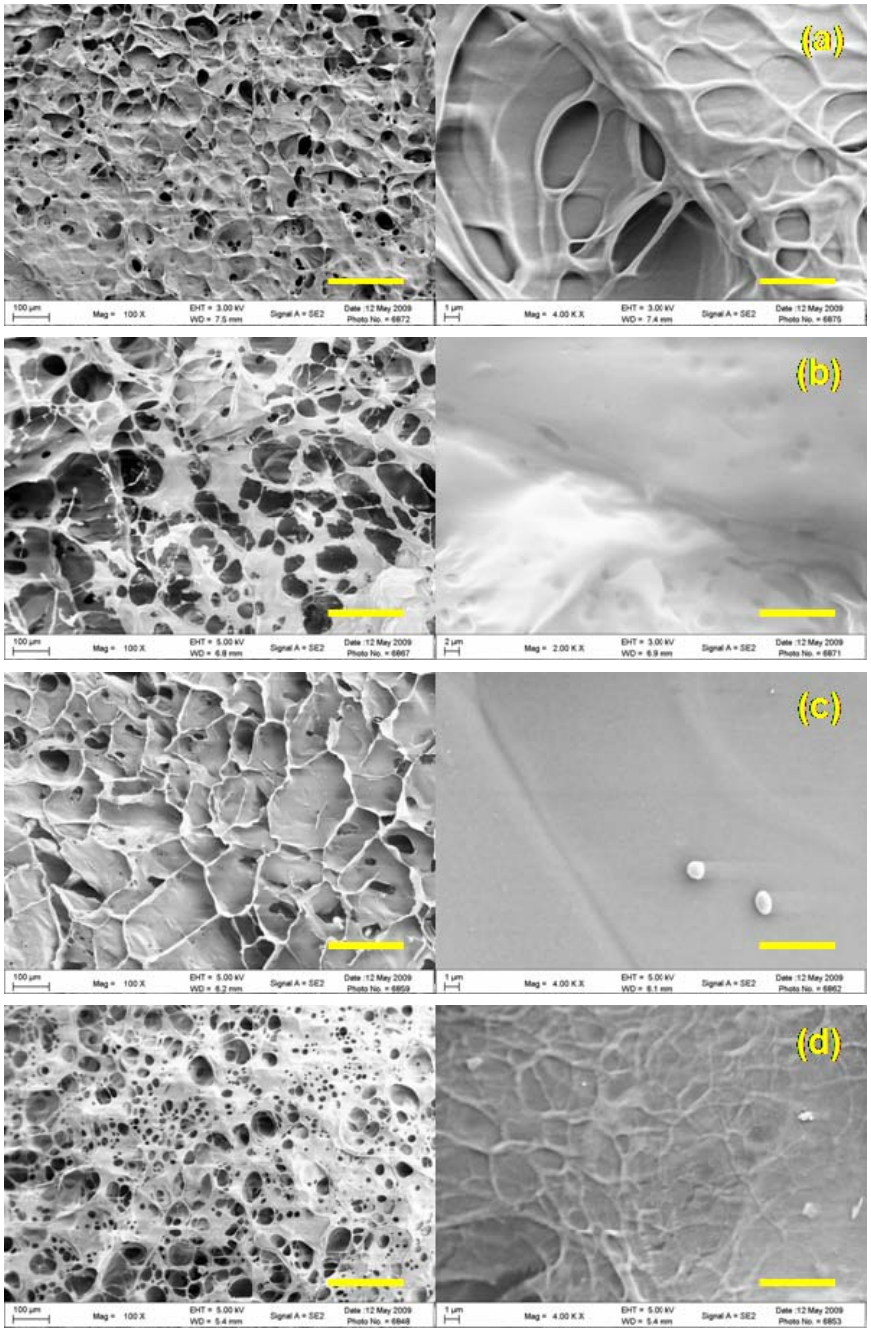

100X 4000X

before rinse

Figure 2.5 SEM microscope images showing the structure of hydrogels: (a) plain agarose; C-A hydrogels before and after neutralization: (b & e) 0.33%, (c & f) 1.0% and (d & g) 2.0%. 100X: scale bar = 200 μm; 4000X: scale bar = 5 μm.

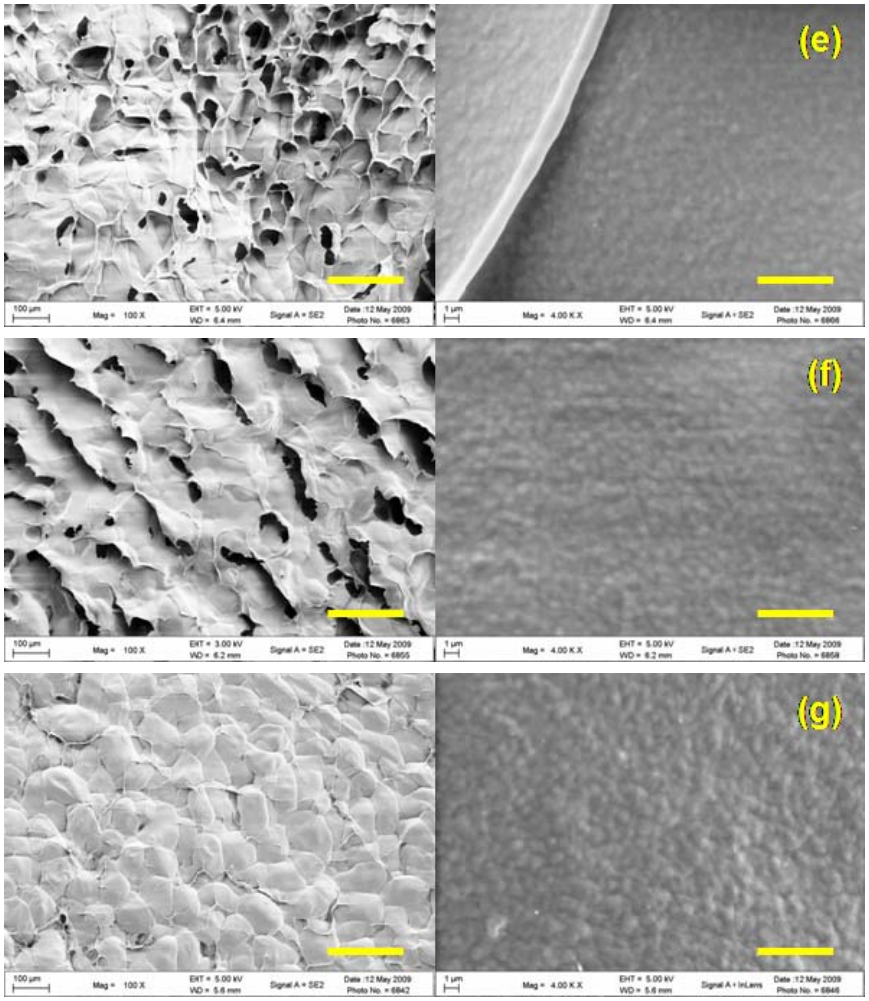

100X 4000X

after rinse

Figure 2.5 continued.

A hydrogels form partially or fully closed structure. Higher magnification images (4000X) reveal a relatively smooth structure for non-rinsed C-A hydrogels and grainy structure for rinsed samples.

These observations can be attributed to the phase separation of chitosan in the neutralized hydrogels (**Fig. 2.6**). Briefly, the chitosan used in this study is only soluble in acidic solutions (pH $<$ 6.5) due to the electrostatic effect among the protonated amine groups along the polymer chains.[2] Under this condition, the C-A hydrogel forms a homogeneous phase with extended chitosan chains within the agarose matrix and displays a clear appearance. The electrostatic effect, however, is diminished in neutral environments because most of the amine groups are deprotonated when pH values approach 7.4.[72] Therefore, the extended chitosan chains contract after neutralization, and aggregates of chitosan precipitated within the agarose matrix, resulting in the phase separation.[3] We have observed with a light microscope a uniform distribution of the chitosan aggregates throughout the entire depth of the gel, indicating a well-dispersed precipitate. It is also worth noting that the size of the chitosan aggregates (average estimated diameter of 1 μm from SEM images) did not change much as the concentration of chitosan increased. The apparent increase in opacity and the number of aggregates could be accounted for by the higher concentration of chitosan.

2.3.3.3 Neuron adhesion on C-A

There was a significant difference in the number of live cells between hydrogels with and without chitosan. All of the C-A hydrogels showed better support of neuron adhesion than the plain agarose hydrogel (**Fig. 2.7**). As mentioned earlier, this difference is most likely due to the ability of chitosan chains to interact with the cell membrane by electrostatic effect. Similar results have also been reported for other types of cells, indicating a nonspecific interaction. It is quite difficult to measure the surface potential of the hydrogels due to their low stiffness. However, previous studies have already shown that even though most of the amine groups are deprotonated in a neutral environment, there are still positive charges on the surface of neutralized chitosan films[49] and microspheres[13].

Since chitosan can enhance the adhesion of neurons, one would expect a simple linear relationship between the cell density and the chitosan concentration in the hydrogel. However,

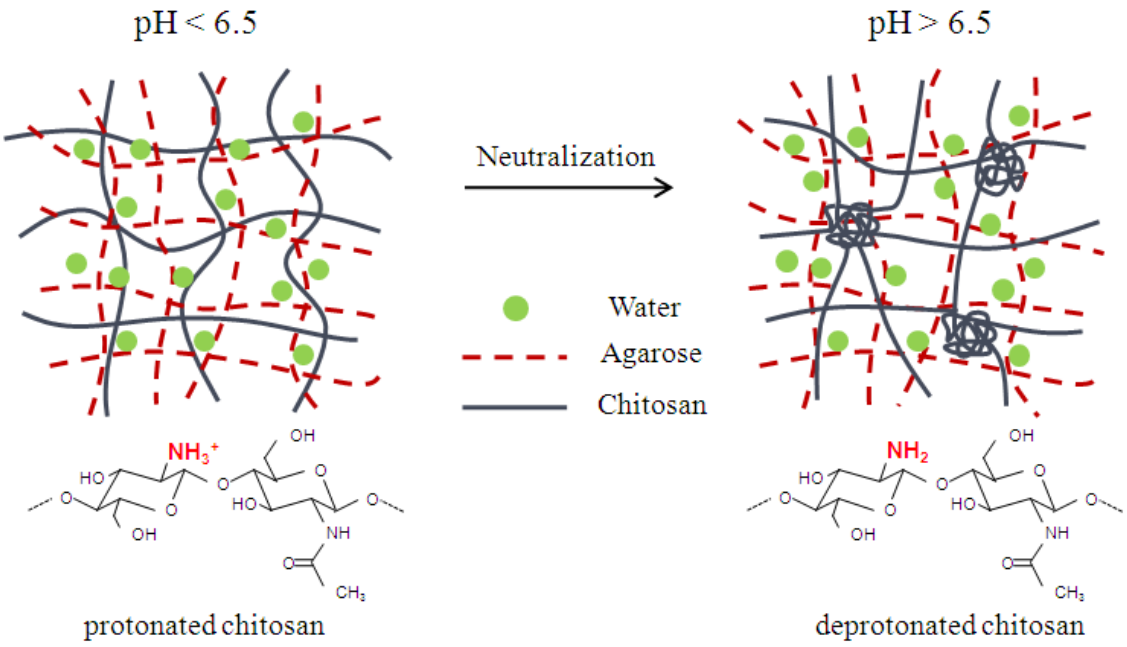

Figure 2.6 Schematic of phase separation of C-A hydrogel as a result of neutralization. Corresponding chemical structure change of chitosan due to the pH change of the solvent is also given.

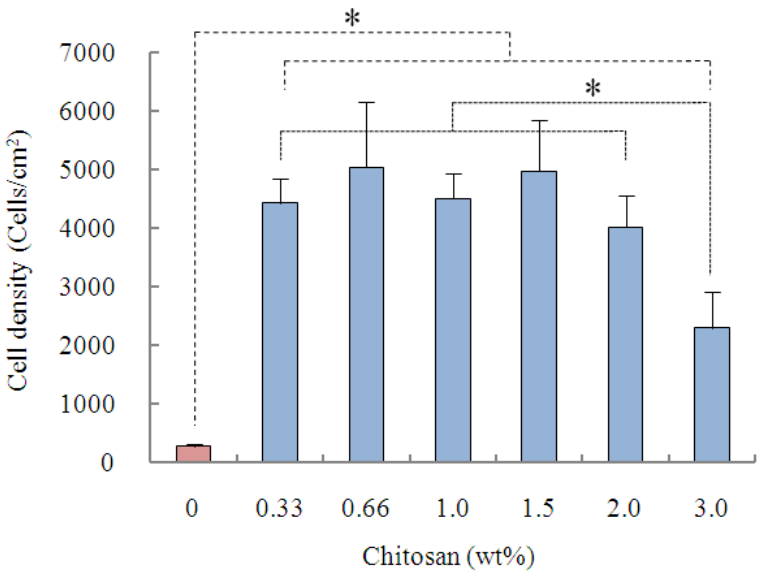

Figure 2.7 Cell density versus chitosan concentration in C-A hydrogels. Error bar = standard deviation (n = 3, *$p < 0.05$).

this is far from the case. There was no significant difference in the cell density on the C-A hydrogels within the concentration range of chitosan in this study, except the 3.0% C-A composition (**Fig. 2.7**). Considering the size of the cell body (~15 μm) and chitosan aggregates (~1 μm), it is reasonable to conclude that a single cell can interact with several chitosan aggregates at the same time, and as long as sufficient chitosan is added, the change of chitosan concentration would not influence the total number of cells attached on the substrates. This observation is similar to studies demonstrating a surface cell-adhesive RGD ligand density threshold, where increases in the RGD density did not significantly affect the number of cells attached, suggesting a saturation of receptor-ligand bonds at higher ligand density.[73] The number of neurons attached on the 3.0% C-A gel is statistically lower than the rest of C-A compositions. It could be due to the fact that the gel supported relatively poorer neurite development (as discussed next) and therefore, a portion of the loosely adhered neurons died during culture or lost during the staining process.

2.3.3.4 Neurite extension on C-A

For a substrate to be effective as a scaffold for neural tissue engineering, it should not only support neuron adhesion, but also support neurite extension. Neurites are very important projections of a neuron, as they will lead to the eventual formation of functional neural network and enable synaptic transmission. It is therefore essential to examine how the C-A hydrogels affect neurite outgrowth. Significant differences were observed for the ability of neurons to develop neurites on different C-A hydrogels (**Fig. 2.8**). The percentages of cells that could develop neurites longer than 50 μm (50-150 μm & >150 μm) after a 3-day culture on 3.0% C-A gels were much lower than the others, and 2.0% formulation also lacked the ability to support very long neurites (>150 μm). Such inhibition effect from substrates fabricated to facilitate neurite extension has been observed in an earlier study on polylysine-functionalized chitosan hydrogels.[6] Crompton et al. found that immobilized poly-D-lysine (PDL) improved cell survival up to an optimum concentration of 0.1%, and further increases of PDL resulted in a decrease in cell number and neurite outgrowth. The authors attributed this result to the strong interaction of cells with PDL in their 3D gel. We are proposing an alternative hypothesis to explain the phenomenon observed in the present study. Our hypothesis is based on our observations from

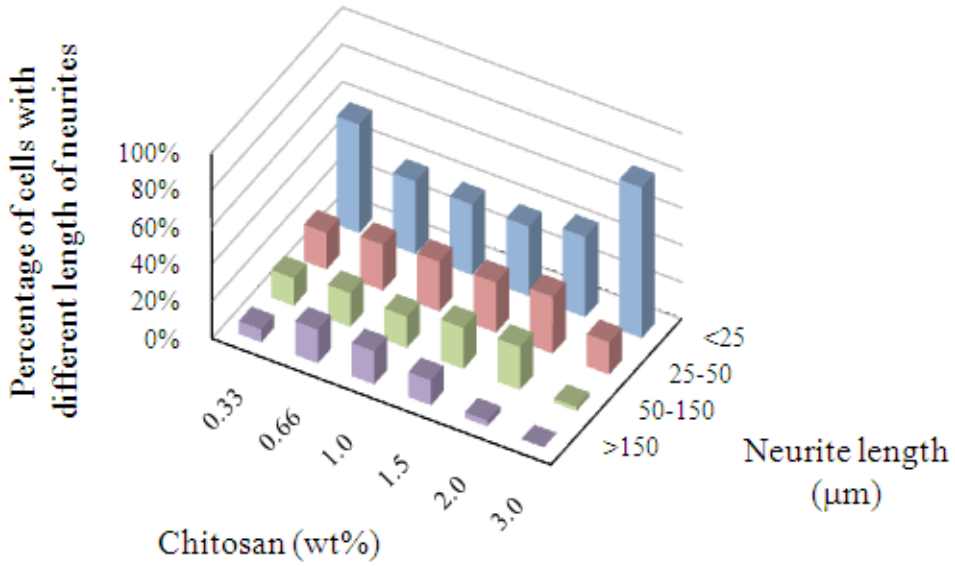

	0.33	0.66	1	1.5	2	3
>150	7%	18%	18%	13%	3%	0%
50-150	15%	18%	17%	22%	23%	2%
25-50	20%	25%	27%	27%	31%	17%
<25	58%	39%	38%	38%	43%	81%

Figure 2.8 Percentages of neurons with different lengths of neurite versus chitosan concentration.

neuron differentiation and morphology study, which will be further discussed in the following section.

2.3.3.5 Neuron morphology on C-A

Neurons on all C-A hydrogels exhibited a 3D profile, as shown from the confocal images where the cell body of the neuron situated at the surface of the gel and the neurites were seen extending into the gel towards the bottom (**Fig. 2.9 & Fig. 2.10**). It indicated that the neurite-permissive property of the agarose scaffold was preserved despite the addition of chitosan. However, cells on C-A hydrogels with lower chitosan concentration (0.33%, **Fig. 2.10 (a)**) tended to extend axons, typically the longest neurites, as a straight line without obvious branching. Their counterparts on denser gels (1.0%-3.0%) favored tortuous axon morphology with extensive branches (**Fig. 2.10 (b) – (d)**). This trend can also be seen on the confocal images showing the overall feature of the network, although the fine structure of the neurites was not visible under such low magnification (**Fig. 2.9**). Data for 0.66% and 1.5% C-A hydrogels were not shown as the neurons on these two compositions exhibited similar properties as the 1.0% formulation.

Why do neurons behave so differently on the simple blends of chitosan and agarose? In order to answer this question, neuron differentiation was "simulated", by hand, in two-dimensional (2D) mimic structures of different C-A hydrogels (**Fig. 2.11**). The basis for this simulation is the observation that chitosan aggregates in these C-A hydrogels are relatively uniform in size (~1 μm) and randomly distributed (**Fig. 2.4 (b)**). Briefly, different percentages of random dots (1 unit) in a blank area (100×100 units), corresponding to different chitosan concentrations, were generated using Matlab. Neurites can only pass through the white area, which represents the permissive agarose matrix. However, attaching a black dot (chitosan aggregate) at each step is necessary for neurite extension. The distance between two steps must be shorter than 6 units (6 μm), which is the reported critical bridge distance for the growth cone at the end of an axon to migrate.[74] Branching is preferable when the neurite has to make a sharp turn. Although the "simulation" work was done in a 2D manner, the results shared quite similar profiles with the neurons from the real confocal microscopy images (**Fig. 2.10**), reflecting the

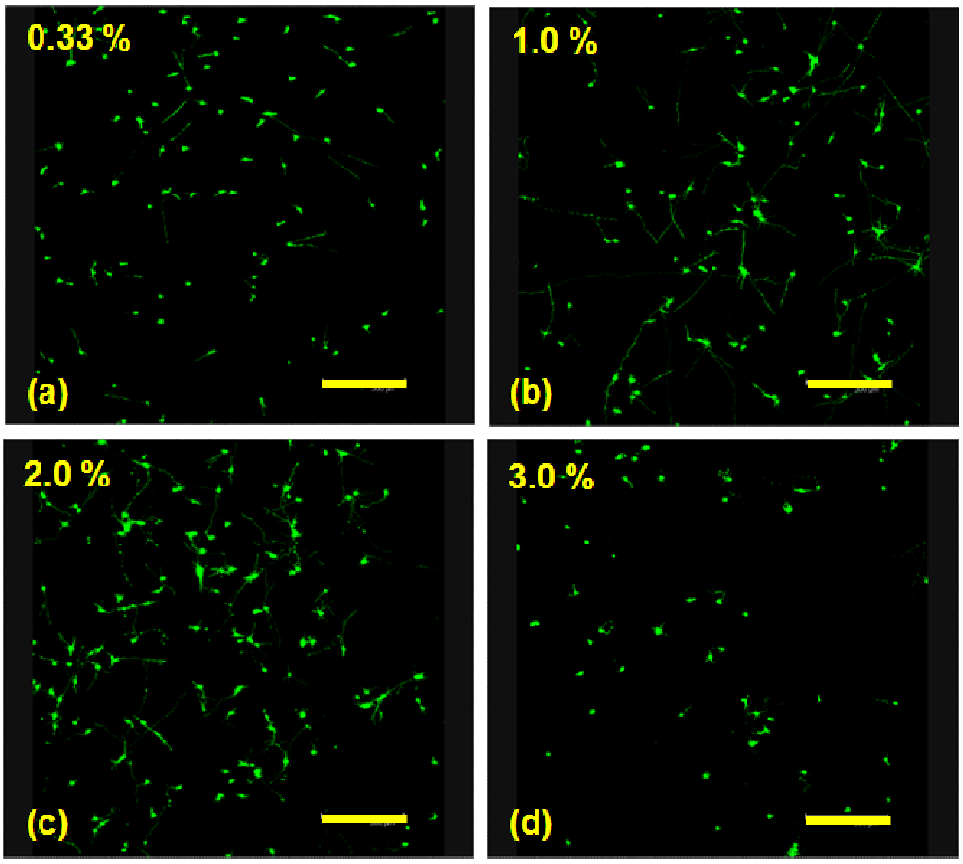

Figure 2.9 Confocal images of the neuron network on C-A. The highest depth neurites could reach is 160 μm below the surface according to our observations. Scale bar = 300 μm.

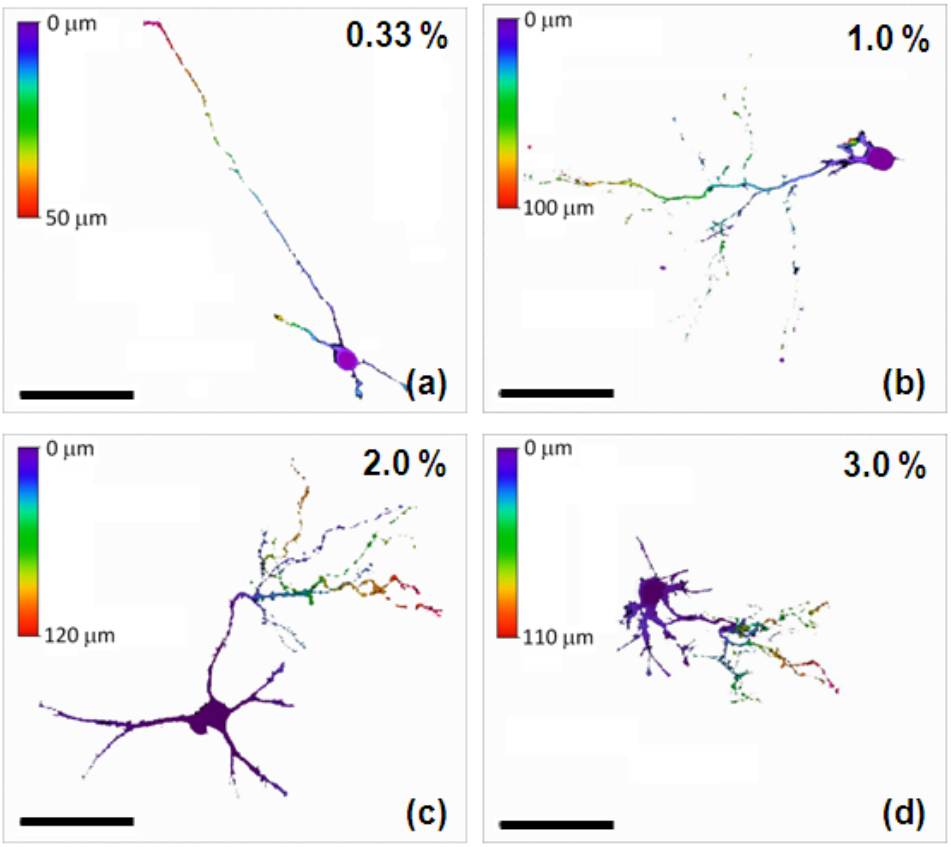

Figure 2.10 Representative images showing neuron morphology on C-A. Color band indicates the depth of the neurite location. Scale bar = 50 µm.

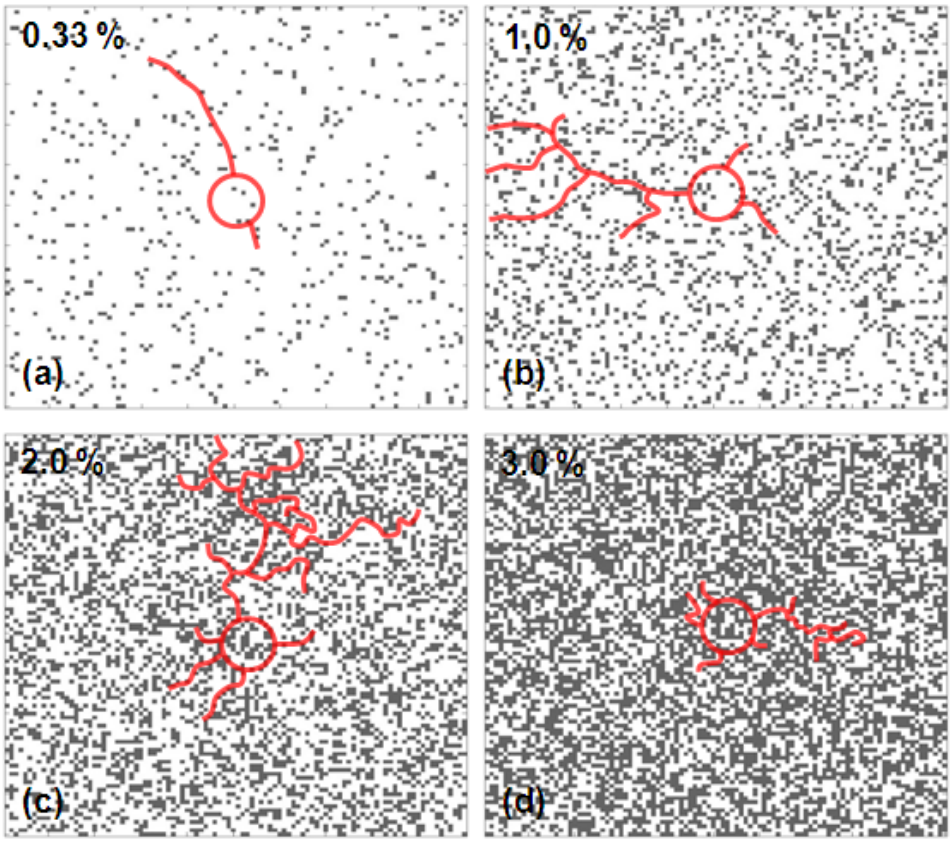

Figure 2.11 ”Simulation” of neurite differentiations: simulated by hand on substrates mimicking the hydrogels using random dots generated by Matlab.

two-fold functions of chitosan aggregates during neuron differentiation: “adhesion sites” and “steric hindrances”.

On the one hand, the positive charges on the chitosan aggregates support neurite attachment during differentiation. According to the study by Clark et al.,[74] the distance between two attachment sites needs to be less than 6 μm to guarantee a successful forward procession for growth cones. Because even the hydrogel with the lowest concentration of chitosan (0.33%) is able to support neurons to develop fairly long neurites, it is reasonable to conclude that all of the concentrations of chitosan are sufficient for satisfying the minimum gap distance for the growth cone to move forward. Light microscopy images also show such a network with a comparable inter-aggregate distance (**Fig. 2.4 (b)**).

On the other hand, the chitosan aggregates are formed by highly contracted polymer chains, so it is not easy for neurites to penetrate these dense areas. When growth cones meet such a “roadblock”, it is more favorable for them to make a turn and/or branch out to continue their pathfinding. The more concentrated the C-A hydrogel, the higher possibility for the growth cone to encounter a hindrance and make turns and branches. These side branches of neurites, also known as collaterals, are quite favorable because they can form points of contact with appropriate target neurons and provide more chances for signal transmission among neural cells. However, the continuing increase of the chitosan concentration could have its drawbacks, causing the chitosan aggregates to block neuronal outgrowth. We thus hypothesize that it is this steric hindrance effect that caused the 3.0% C-A hydrogel to perform poorly for neurite extension even though it should have the most attachment sites for neurons.

The two functions of chitosan play very important roles in enhancing neuron attachment and guiding neurons to develop multi-branching neurites in a 3D manner, resulting in the formation of a more extensive network and better communication among neural cells (**Fig. 2.9**). The C-A hydrogel, taking advantage of the permissive structure of agarose hydrogels and the two-fold properties of chitosan, can be a promising tissue scaffold for brain injury repair. Based on our study, the optimum concentration of chitosan in the agarose gel is 0.66-1.5 wt%, which supports more cells with longer neurites and better neural network compared with the other compositions (**Fig. 2.8 & Fig. 2.9**).

Although a few studies have previously reported that high substrate density can inhibit nerve growth,[75, 76] our work is the first one to demonstrate such an inhibition effect by correlating the morphology of single cells and a 3D structured tissue scaffold. This hypothesis not only explains our observations in the cell culture study, but also helps us better understand the mechanism by which a neurite extends or branches.

2.4 Conclusions & Significance

A simply prepared C-A hydrogel system was developed for TBI repair. The stiffness of the C-A hydrogels was very similar to the brain tissue, providing a mechanically compatible environment for neuron growth. The agarose matrix presented a permissive structure for neuron growth, and its incapacity for neuron adhesion was complemented by the addition of chitosan. More importantly, a novel hypothesis on the "steric hindrance" effect of chitosan on neurite outgrowth was proposed based on our observations. It implies that a proper adjustment of the chitosan concentration could directly impact the morphological development of neurons, and could be used as a simple yet versatile approach to obtain desirable neuronal structures. This hydrogel system and its multi-functionality allow for applications of simply prepared agarose-based hydrogels for neural tissue repair.

CHAPTER III

GRAPHENE-CHITOSAN NANOCOMPOSITES FOR NEUROPROSTHETICS

A manuscript presenting part of the data in this chapter has been submitted to Nano Letters for review in March of 2010 [Zheng Cao, Yongchao Si, Craig Cavanaugh, Wei He. Graphene-chitosan nanocomposite for neural interface applications]. Submitted data include: Fig. 3.2, Fig. 3.3, Fig. 3.4 (a, e and f), Fig. 3.5, Fig. 3.6, Fig. 3.7, and Fig. 3.8 (a, c, e and f). Section 3.1, 3.2.3 and 3.3 are mostly cited from the submitted manuscript with a few modifications. Section 3.2.1 and 3.2.2 are newly written.

The first author (Zheng Cao) finished all of the experiments in this study. The fourth and corresponding author (Dr. Wei He) is advisor of Zheng Cao and financially supported this work. The second author (Dr. Yongchao Si) and (Dr. Craig Cavanaugh) are collaborators of Dr. Wei He, and provided the graphene solution and professional advice for this work.

3.1 Introduction

Successful interfacing with neural tissue holds enormous potential for both fundamental neuroscience research and clinical treatment of neurological diseases or injury.[77-82] A key component of this application is the implantation of the device in neural tissue to exchange information with local population of neurons. Currently, these implantable devices suffer from large variability and limited longevity in performance, which is one of the major bottlenecks for neural interface technology.[78, 79, 82] To address this challenge, the neural interface community is exploring novel implantable materials.[48] In this study, we rationalize that graphene-based materials could potentially be used for implantable neural devices.

Graphene (G), a 2-D monolayer of carbon atoms covalently-bonded in a hexagonal array, is being intensively studied since the discovery of processes enabling the exfoliation of G into its free-standing form.[83] Its excellent properties, including high values of electrical conductivity,[84] thermal conductivity,[85] and specific area,[86] make it a promising candidate in a variety of applications, such as energy storage materials,[86] polymer composites,[87, 88] liquid crystal

devices,[89] etc. Unlike carbon nanotubes (CNTs), its sibling in the family of carbon materials, very limited study has been reported on the applications of graphene in biomedical fields.[90, 91] Use of CNTs for biomedical applications, particularly those involving placement inside the body, faces a toxicity issue. Studies have reported that CNTs may insert themselves between the lipid bilayer of cell membrane, leading to membrane disruption and cell death.[92-95] Toxicity issues also arise from the intrinsic impurities from the catalysts used for CNT production.[96-98] Although graphene sheets are ultra-thin (~1 nm), a relatively large lateral size (several micrometers) on the 2D plane is achievable.[99] This could result in less size-induced toxicity than CNTs. Furthermore, graphene production is less plagued with impurity issues,[100] which benefits biomedical applications.

Currently, four methods have been used to prepare graphene: chemical vapor deposition (CVD) and epitaxial growth, micromechanical exfoliation of graphite, epitaxial growth on electrically insulating surfaces, and creation of colloidal suspensions.[100] Among these methods, production of graphene from colloidal suspensions is the most scalable and versatile approach. This allows for potential mass production and a variety of chemical functionalizations. Typically, graphene cannot be easily dispersed in water, which is the most preferred solvent for biomedical applications. This challenge has been addressed by the development of water soluble graphene with the introduction of sulfonate groups, which can be readily dispersed in water at reasonable concentrations (2 mg/mL) with its electrical conductivity preserved.[99] It provides an opportunity to explore the biomedical potentials of graphene.

Graphene is non-biodegradable, thus suitable for long-term in vivo applications. It is also electrically conductive, thus able to provide a communication platform with neurons. To improve its interaction with neurons, we complemented graphene with chitosan (C), to form a nanocomposite. Results from Chapter II have shown that inclusion of chitosan can significantly improve neuron adhesion to substrates. In this chapter, graphene-chitosan (G-C) nanocomposites were prepared and characterized for properties pertinent to neural interface applications.

3.2 G-C Nanocomposites for Neuroprosthetics

3.2.1 Rationales

This section briefly introduces the rationales behind the experimental design and special techniques used in this chapter. Please see *section 3.2.2 Experiments* for detailed experiments.

3.2.1.1 Sample preparation

The concentration of chitosan is the only variable in sample preparation. A stock chitosan solution was prepared first, and added into graphene later. A graphene stock solution (0.5 mg/mL in DI water) was directly provided by our collaborator Dr. Craig Cavanaugh and Dr. Yongchao Si from University of North Carolina at Chapel Hill. A consistent graphene concentration (0.4 mg/mL) was maintained for all the G-C solutions. Although both coatings and free standing films can be prepared by air evaporation of the G-C solution, G-C coatings on glass will be used for most of the study due to its ease of preparation and handling. These experiments include: electrical property, surface morphology and topography, neuron adhesion, and neuron morphology.

The flexibility of G-C was examined by rolling the free standing film up. An insertion test was done to show its feasibility for surgical implantation.

3.2.1.2 Sample characterization

The remarkable electrical conductivity of graphene is one of the main rationales behind this study. Because chitosan is non-conductive, the electrical property of G-C needs to be confirmed first. The electrical resistance of G-C was measured using a multimeter.

The surface topographical features can have great influence on cell adhesion and growth.[101] Therefore, two methods (SEM and AFM) were selected in this chapter to characterize the surface structure of G-C samples. Typically SEM can only detect information at the micro-scale due to its limited magnification, but a large area could be scanned at one time. AFM, on the other hand, could provide nano-scale information but with a relatively small scanning area. Results from these two methods could give us a comprehensive idea about the structural properties of the sample surface. The roughness of the surface can also be calculated using the software provided by the AFM vendor.

3.2.1.3 Biocompatibility of G

Good biocompatibility is one of the most critical features that a biomaterial should possess. As mentioned earlier, graphene could have lower cytotoxicity due to its large lateral size on the 2D plane. Typically there are two ways to evaluate the biocompatibility of a film substrate. One way is directly seeding cells on the fabricated substrate and assessing the cell viability after culture. Another way is culturing cells on a good substrate using growth medium supplemented with the raw material used for the substrate fabrication. The second method was applied in this study because it can reflect the toxicity of single graphene sheets on cells.

To compare our results with a previous work studying the cytotoxicity of CNTs,[98] we employed a fibroblast cell line (NIH 3T3) in this study. A relatively high treatment concentration (25 μg/mL) was selected for the culture. Besides, a neuron cell line (N2a) was also used for cytotoxicity study, since this study is designed for neural engineering applications.

3.2.1.4 Neuron responses to substrates

Since this G-C nanocomposites system is newly developed, both cell line (N2a) and primary cortical neurons were used for neuron adhesion study. Due to their different characteristics, different culture times were employed. Because N2a can attach easily on many substrates and proliferate quickly in serum-supplemented medium, a relative short culture period (4-hour) was chosen for culture. On the contrary primary cortical neurons only attach on specially treated substrate and don't proliferate during culture, a longer culture period was used. A poly-L-lysine (PLL) coating on glass was used as a positive control. All cell adhesion data were normalized as percentages to PLL.

Like the C-A hydrogel study, neurite outgrowth was also evaluated for primary culture. A different technique was used here for the following reasons. The highest magnification lens of the confocal microscope used in this study is 63X, with which we cannot see much detail related to the interaction between neurons and the substrate. Because the G-C coatings are dark in appearance, a conventional inverted light microscope cannot be used for observation. SEM imaging, due to its high magnification and easy imaging on sample surfaces, was used for neuron morphology characterization in this study. Because the glass supported G-C coatings are dry and rigid, SEM fixation is feasible. The reason that we did not use this method for the hydrogel study

is because there is a concern about the dehydration process in the SEM fixation, which may destroy the hydrogel structure and the interaction between the cells and substrate. Because cells are not conductive, a gold sputter coating needs to be applied on the samples before imaging.

3.2.2 Experiments

3.2.2.1 Preparation of G-C

Chitosan was firstly dissolved in a 2.0 wt% acetic acid solution to a final concentration of 16 mg/mL. A series of G-C solutions (weight ratio: 1:0, 1:0.5, 1:1, 1:4 and 1:8) were prepared with graphene suspension (0.5 mg/mL, Allotropica Technologies), DI water and the chitosan stock solution. A consistent graphene concentration (0.4 mg/mL) was maintained for all formulations. **Table 3.1** shows the formulations for all samples prepared.

Stability of the G-C dispersions was examined by visual inspection after 24 h of sitting. Supported G-C nanocomposite films were prepared by evaporation on glass. Briefly, 100 μl dispersion of G-C was casted on substrates and allowed slow evaporation overnight at room temperature. Thin free standing G-C films were prepared on poly(dimethyl siloxane) (PDMS) in the same way, except larger volume of dispersions were used.

3.2.2.2 Electrical property of G-C

The resistance of both plain graphene (PG) and G-C composite films was measured using a multimeter (Resistivity Meter SRM-232, Guardian Manufacturing Inc.) to determine if the electrical characteristic of graphene is lost after the addition of chitosan, a non-conductive polymer.

3.2.2.3 Surface morphology and topography of G-C

The surface and cross-sectional structure of the nanocomposite films was characterized with SEM. Atomic force microscope (Agilent AFM 5500) measurement was performed in contact mode for nano-scale characterization on the surface of uniform films. Both average and root mean square roughness can be calculated using the customized software of the AFM.

Table 3.1 Formulations for G-C Nanocomposites

Sample	Final concentration (mg/ml)		Solution volume (ml)		
	G	C	G (0.5 mg/ml)	C (16 mg/ml)	DI H_2O
PG	0.4	0	0.8	0	0.200
G-1-C-0.5	0.4	0.2	0.8	0.012	0.188
G-1-C-1	0.4	0.4	0.8	0.025	0.175
G-1-C-4	0.4	1.6	0.8	0.100	0.100
G-1-C-8	0.4	3.2	0.8	0.200	0

3.2.2.4 Cytotoxicity of G

Culture medium for NIH 3T3 is Dulbecco's modified Eagle's medium (DMEM) supplemented with 10% Hyclone FetalClone III (Thermo Scientific), 1% penicillin/streptomycin (P/S) and 1% L-glutamine. Medium for N2a culture DMEM supplemented with 10% fetal bovine serum (FBS), 1% P/S, and 1% L-glutamine. Cells were seeded on 48-well plates (1×10^4 cells/cm^2) and cultured in medium. After a 4-hour incubation at 37 °C in a humidified 5% CO_2/95% air atmosphere, half of the cultures was treated with graphene solution to a final concentration of 25 μg/mL.[98] The cells were cultured for another two days. Then the viability of cells was characterized using WST-1 assay (Roche) following the recommended procedure by the manufacturer. The absorbance was measured using an ELISA plate reader at 450 nm.

3.2.2.5 Neuron adhesion on G-C

As N2a can attach easily on many substrates and proliferate soon in serum-supplemented medium, a relative short culture period (4-hour) was chosen for culture (seeding density: 4×10^4 cells/cm^2). Primary cortical neurons were harvested from 9-day-old chicken following the procedure described earlier (*section 2.3.2.4 Primary cortical neuron culture on C-A*). Because primary cortical neurons do not proliferate, a 5-day culture was used for both cell adhesion and morphology study (seeding density: 2×10^4 cells/cm^2).

At the end of the cultures, cells were live stained with 0.05 v/v Calcein AM solution in PBS and incubated at 37 °C for 20 min. Samples were rinsed twice with PBS before and after fluorescence staining. Fluorescence images were taken using the confocal microscope. Neuron adhesion on the substrates was assessed by counting cell number using Image J. The results were expressed as percentage to the PLL positive control.

3.2.2.6 Neuron morphology on G-C

Primary cortical neuron was cultured for neuron morphology study. After the fluorescent imaging, cultures were fixed and dehydrated. Briefly, cells were washed twice with 0.1 M Millonig's phosphate buffer (Electron Microscopy Sciences), followed by primary fixation with 3% glutaraldehyde (Electron Microscopy Sciences) in the same buffer for 1 hour at room temperature. Then cells were rinsed with buffer for 3 times (10 min each). Secondary fixation

was performed for 30 min with 1% osmium tetroxide (Electron Microscopy Sciences). Cell dehydration was carried out using ascending grades of ethanol (25%, 50%, 75%, 95%, 100%, and 100%) for 10 min at each grade. Subsequently, samples were immersed in the mixtures of ethanol and hexamethyldisilazane (HMDS) with a descending order of ratio (ethanol: HMDS = 2:1, 1:1, and 1:2), followed by 100% HMDS dehydration twice for 10 min each. Samples were vacuum dried and kept in a desiccator to ensure a complete evaporation of HMDS. For imaging, samples were mounted on aluminum stumps, coated with gold in a sputtering device, and examined by SEM.

3.2.2.7 Statistics

The same technique as described in *section 2.3.2.8 Statistics* was used for statistical analysis.

3.2.3 Results & Discussion

3.2.3.1 Preparation of G-C

A prerequisite for the preparation of a uniform film is an even dispersion of the source solution. As shown in **Fig. 3.1 (a)**, solutions of plain graphene (PG), G-C composites with graphene to chitosan ratios of 1:4 (G1C4) and 1:8 (G1C8) were stable and well-dispersed after 1 day or longer, while G-C composite with graphene to chitosan ratio of 1:0.5 (G1C0.5) and 1:1 (G1C1) precipitated at the same time point. Obvious aggregates were observed right after the mixing of graphene and chitosan solution for G1C1.It has been suggested that the repulsive electrostatic force between the negatively charged graphene sheets (**Fig. 3.2**) accounts for the stability of the PG dispersion.[99] In this case, the introduction of positively charged chitosan solution likely neutralized the negative charges on graphene, resulting in the collapse of the graphene dispersion (G1C1). When less chitosan is added, the graphene is not totally neutralized, resulting in a partially precipitated solution (G1C0.5) (**Fig. 3.1 (b)**). When additional chitosan is added, the final solution becomes well-dispersed again (G1C4 and G1C8), most likely due to the positive charge from the excess chitosan. The exact mechanism underlying the interactions between graphene sheets and molecular chains of chitosan is yet to be elucidated, but we did notice a darker appearance for G1C8 compared with other compositions, even though all samples

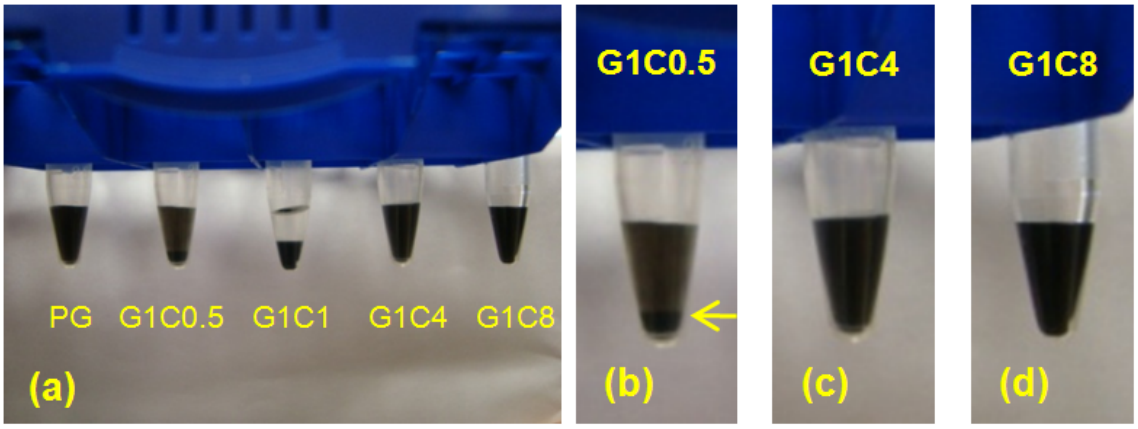

Figure 3.1 Photograph of G-C dispersions: (a) at various ratios of graphene to chitosan; (b) partially precipitated G1C0.5 solution after 1 day sitting; (c) & (d) the darker appearance of G1C8 compared with G1C4.

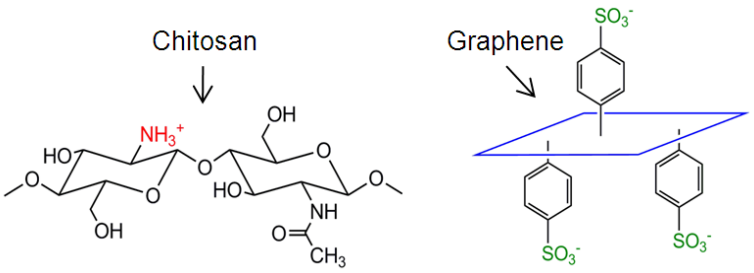

Figure 3.2 Chemical structure of chitosan and water soluble graphene.

should have the same amount of graphene (**Fig. 3.1 (c) & (d)**). It would be informative to uncover the microstructures of the components in the G-C solutions in future studies.

A free standing film was prepared by evaporating G1C4 solution on a PDMS block. The films can be easily peeled off the PDMS and rolled up (**Fig. 3.3 (a) - (c)**), demonstrating good flexibility. This is a desirable feature for implantable neural prosthesis.[102, 103] It was also confirmed that the G-C films are mechanically strong enough for insertion, by testing with an agarose gel mimicking brain tissue (**Fig. 3.3 (d)**).

3.2.3.2 Electrical property of G-C

The G-C films remained electrically conductive, with resistance lower than that of a silicon wafer (**Table 3.2**). As expected, the G-C nanocomposites were less conductive than the PG, and the more chitosan in the composite, the higher the resistance. The ability of graphene to impart electrical properties to non-conducting polymer is consistent with previous reports of electrically conductive polystyrene-graphene composite material.[87] Though we demonstrated that the G-C nanocomposites can be electroactive, the G : C ratio in the nanocomposite requires further optimization in order to achieve an electrical property suitable for neural interfacing.

3.2.3.3 Surface morphology and topography of G-C

Surface properties play critical roles for biomaterials. Specifically, surface morphology directly impacts cellular interactions with the biomaterial. Scanning electron microscope (SEM) images show the surface morphology of the supported films and the cross-section structure of a free-standing G1C8 film (**Fig. 3.4**). A drastic change in morphology can be seen between PG and G-C composites. While PG forms a smooth surface at the micro-scale (**Fig. 3.4 (a)**), G-C composites have a relatively rough surface (**Fig. 3.4 (b) – (e)**). Among G-C composites, the surfaces of G1C4 and G1C8 possess uniform grainy structure (**Fig. 3.4 (d) & (e)**), while G1C0.5 and G1C1 display a surface feature between PG and G1C4 / G1C8 (**Fig. 3.4 (b) & (c)**). The cross-sectional image (**Fig. 3.4 (f)**) shows a continuous internal structure of the nanocomposite, suggesting good percolation of graphene in the nanocomposite. This enables graphene to exert its electrical functionality.

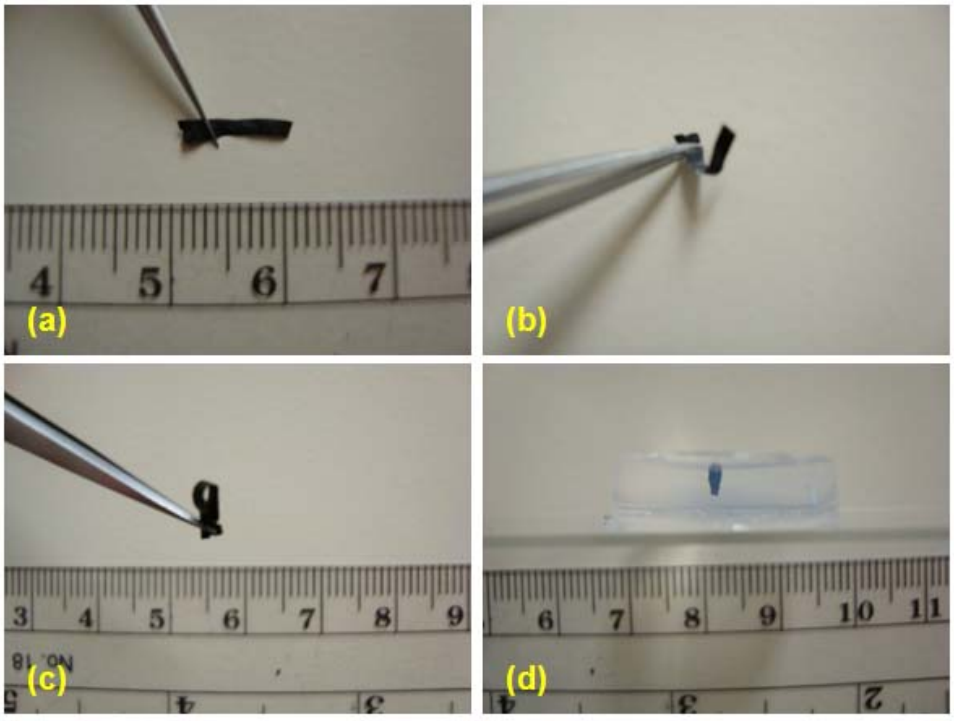

Figure 3.3 Photograph of free standing G-C films: (a) – (c) A free standing G-C nanocomposite films displays flexibility and ease of handling. (d) Insertion test of a free standing graphene-chitosan nanocomposite film with an agarose gel mimicking the brain tissue.

Table 3.2 Electrical resistance of plain graphene (PG), graphene-chitosan composites, and silicon wafer. Data shown as mean ± standard deviation.

Sample	Resistance (kΩ)			Average (kΩ)	Standard deviation
	1	2	3		
PG	1.6	1.2	1.3	1.37	0.21
G1C0.5	9.05	8.68	5.1	7.61	2.18
G1C1	26.73	14.48	19.5	20.24	6.16
G1C4	300	249	230	259.67	36.20
G1C8	2300	1750	2000	2016.67	275.38
Silicon	3612	2587	3248	3149.00	519.62

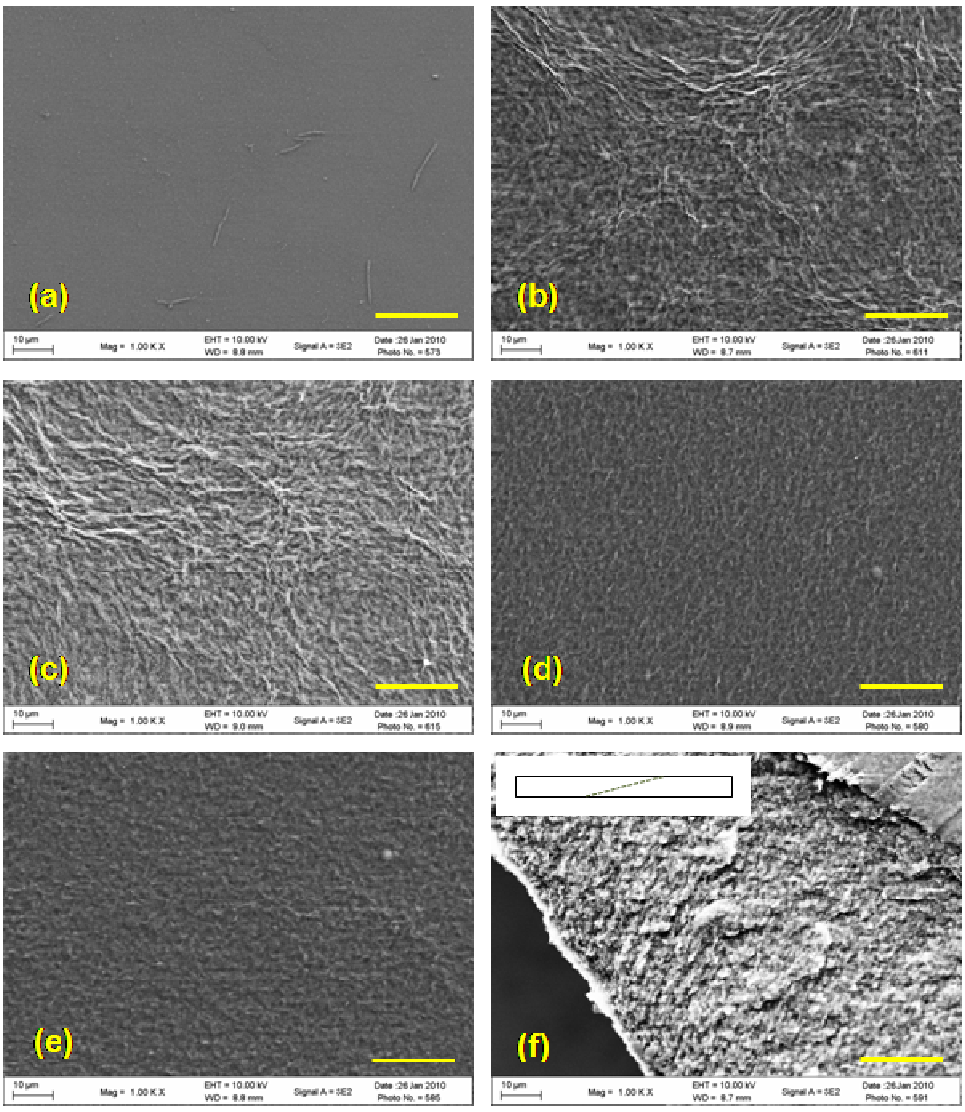

Figure 3.4 SEM images showing the surface morphology of samples: (a) PG, (b) G1C0.5, (c) G1C1, (d) G1C4, (e) G1C8, and (f) the cross-sectional structure of a G1C8 free standing film. The way to prepare the cross section of G1C8 is illustrated on top-left of (f). Scale bar = 20 μm.

Atomic force microscopy (AFM) was used to probe the surfaces of uniform films for calculation of roughness. Nano-scale features were observed on PG surface (**Fig. 3.5 (a)**), with an average root-mean-square roughness of 42 nm. Incorporation of chitosan notably increases the roughness to 137 nm (**Fig. 3.5 (b)**), resulting in a grainy surface. It is interesting that this composite approach changed the nano-structured surface of graphene, which will have implications for subsequent cellular interactions. The topography of a silicon wafer was characterized for comparison (**Fig. 3.5 (c)**).

3.2.3.4 Cytotoxicity of G

As mentioned earlier, cytotoxicity is one of the main concerns in the biomedical applications of CNT, especially for single-wall CNT (SWCNT). Based on their extensive study, Tian et al. attributed the toxic effect of SWCNT to its ultra-small dimensions.[98] Since graphene sheets are two-dimensional materials with micro-scale lateral length, a lower cytotoxicity comparing to CNTs is possible. Compared to the reported 75% survival rate of human fibroblast cells (2-day treatment of SWCNT: 25 μg/mL),[98] a 92.8% survival rate for the same type of cell (2-day treatment of graphene: 25 μg/mL) was observed in our study (**Fig. 3.6**). Graphene also showed high biocompatibility to neuron cells (N2a) with a 93.3% survival rate. The results suggest good cytocompatibility of graphene towards both fibroblasts and neurons and suitable for further investigation for neural interfaces. A recently published article also demonstrates a better biocompatibility of graphene compared with CNTs.[91]

3.2.3.5 Neuronal responses to G-C

Besides electrical properties, good interaction between biomaterials and neurons is particularly desired for neural interface applications. Ideally, the material should support neuron adhesion and growth to ensure high fidelity and maximal signal communication between the implant and the nervous system.

For both the N2a neural cell line and primary chick cortical neurons, PG was not favorable for cell adhesion (**Fig. 3.7**), which could be attributed to the presence of negatively charged sulfonate groups on graphene (**Fig. 3.2**). However, some G-C nanocomposites showed much higher cell attachment (G1C4 for N2a; G1C4 and G1C8 for cortical neuron), suggesting that incorporation of amine-rich chitosan improves the material's ability to support neuron

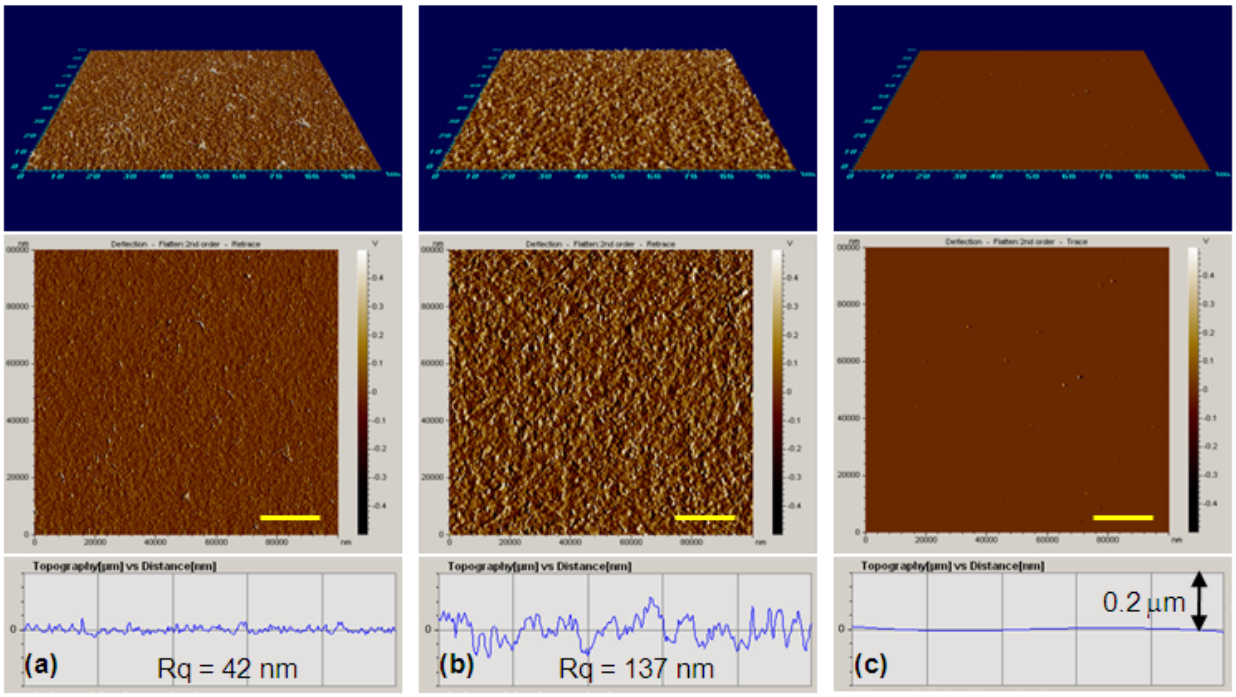

Figure 3.5 AFM images showing the surface topography of samples: (a) PG, (b) G1C8, and (c) silicon wafer. Scale bar = 20 µm.

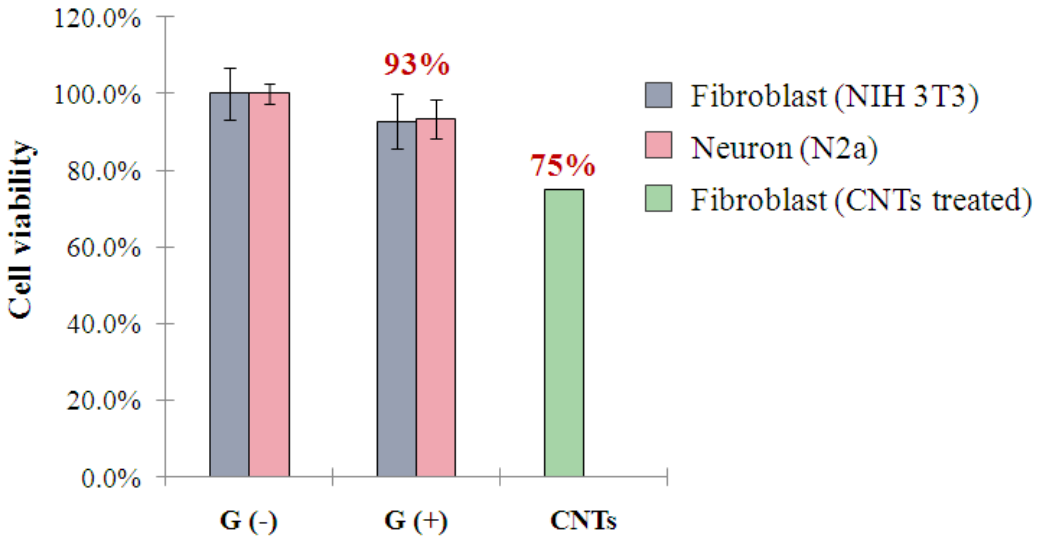

Figure 3.6 Cytotoxicity of graphene (G) showing high survival rate of cells: fibroblast (NIH 3T3 92.8%) and neurons (N2a, 93.3%). Cells were treated with 25 μg/mL of graphene (G+) for 2 days. Control sample without graphene treatment is noted as G (-). The survival rate of fibroblast (75%) with carbon nanotubes (CNTs) treatment is presented for comparison.[98]

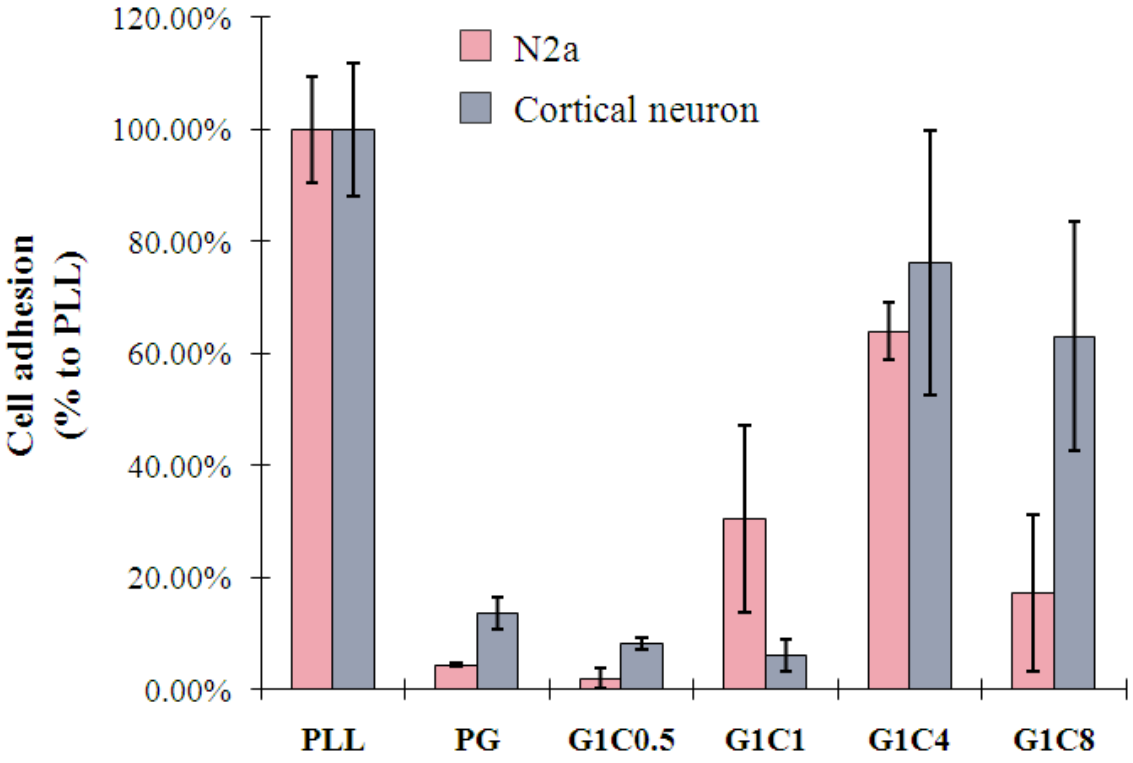

Figure 3.7 Cell adhesion of N2a cell line and primary cortical neuron expressed as percentage to the poly(L-lysine) (PLL) positive control. N2a: G1C4 is significantly higher than other samples; Cortical neuron: G1C4 and G1C8 are significantly higher than other samples. ($n = 3$, $p < 0.05$).

adhesion. The responses of N2a and cortical neuron to this series of G-C composites are slightly different. For example, it appears G1C1 supported more N2a cells, while G1C8 supported more cortical neuron. This observation could be attributed to the different characteristics of the two types of cells.

According to the results from cell adhesion study, the morphology of cortical neuron on PG, G1C4, and G1C8 were investigated by SEM. Extensive neurite-like structures were observed stemming from the body of cortical neurons attached on G-C nanocomposite (**Fig. 3.8 (a)**). This suggests the potential ability of the G-C nanocomposites to induce neural differentiation. It appears as if the surface roughness of the G-C nanocomposites allows for extensive neurite formation (**Fig 3.8 (b) – (d) arrows**). The intimate contact between neurons and G-C surface is advantageous for neural interface applications. It can not only improve neuron adhesive strength to the implanted device and therefore minimize micromotion between the device and the tissue, but also promote signal transduction between the attached neuron and the device. This could lead to enhanced sensitivity of the device. Though PG in general is not pro-neural adhesion, those few cells that did attach were seen with neurite-like structures as well (**Fig. 3.8 (e)**). The morphology of neural processes was very different from those on the G-C surface. The neurites were much fewer in numbers, but they were longer and showed extensive branching (**Fig. 3.8 (f)**). It is as if the cells are trying to maximize the anchoring points with the relatively featureless surface. The long neurites are also beneficial for neural interface applications, as they will allow cell-cell communication. Studies have shown that both micro- and nano-scale topography of the substrates could have influence on cell migration, adhesion, differentiation, and morphology.[104] Although the underlying mechanism remains elusive, the different topographic properties of PG and G-C nanocomposites could account for the different cell morphologies observed in this study. Both morphologies are intriguing and we are interested to further tune the G-C compositions to develop a material that can enable development of both types of neural processes for interfacing.

3.3 Conclusions

We reported for the first time the development of a simple G-C nanocomposite system for potential neural interface applications. The G-C nanocomposites can be prepared both as

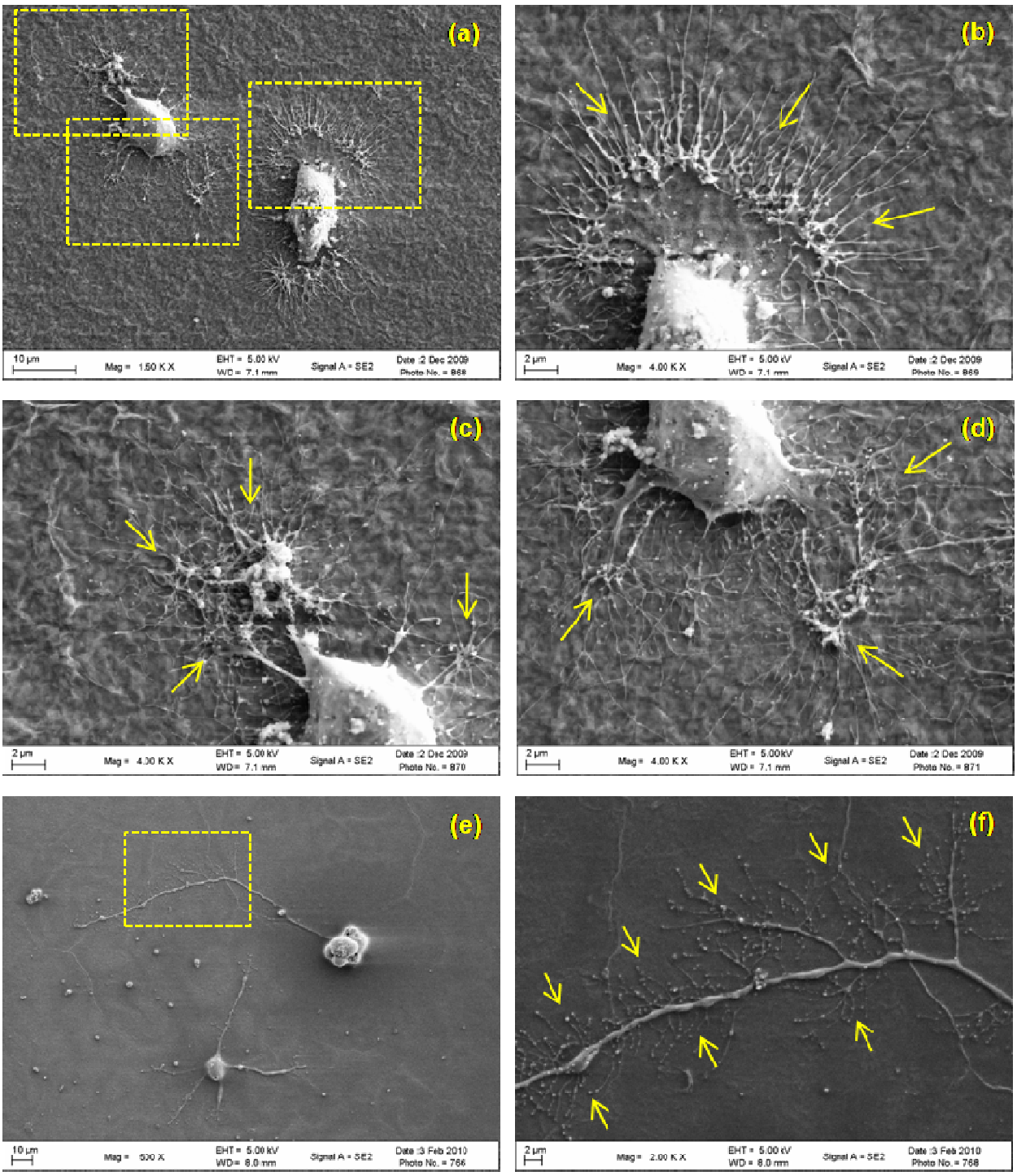

Figure 3.8 SEM images of primary cortical neuron growing on samples: (a-d) G1C8 and (e, f) PG films with different neurite-like structures (arrows).

coatings and flexible free-standing films simply from environmentally and biologically friendly aqueous dispersions of water soluble graphene and chitosan. The free standing films showed good flexibility and capability for insertion. The electrical conductivity of graphene was maintained in the composite system. Cytotoxicity study showed good biocompatibility of graphene towards both fibroblast and neuron. The bio-adhesive property of chitosan was reassured in this study. The morphology of the films was closely dependent on the composition, and directly influenced neuron adhesion and morphology. This biocompatible G-C nanocomposite system is poised for further development and investigation as a novel implantable material to advance neural interface technologies. It could also provide a new platform for in vitro neurophysiology study.

CHAPTER IV
GENERAL CONCLUSIONS AND FUTURE PERSPECTIVES

The ability of chitosan to enhance neuron adhesion was confirmed by the two studies in Chapter II and Chapter III. In respect of the cell morphology, the influences from chitosan were mainly composition dependent:

For the C-A hydrogel system, chitosan was embedded in the scaffold matrix and served as anchorage points for neurite extension. An optimum concentration range of chitosan was found to induce the best neural network compared with other compositions. Neither too low nor too high composition of chitosan could support good neurite outgrowth. A "steric hindrance" effect was proposed to explain the observations, and could be used as a simple yet versatile approach to obtain desirable neuronal structures.

For the G-C nanocomposite film system, the introduction of chitosan affected neuron morphology in another way. A rougher surface with nano-scale features was found for G-C nanocomposite films compared with plain graphene film, likely due to the incorporation of chitosan. Neurons displayed totally different structures on these two types of substrates. The underlying mechanism for this observation is still elusive, but it implies the possibility to tune the topological features of the G-C nanocomposites by simply adjusting the chitosan composition, and eventually control the interaction between neuron and substrates.

To maximize the clinical potential of the C-A hydrogel system, it is important to improve the gelation condition near physiological value. It could be accomplished by either incorporating an enzymatically induced gelation mechanism or tweaking agarose gelation temperature to that near physiological value. Concerns over the slow degradation of agarose and chitosan can be addressed by introducing moieties that allow for controlled release of degradative enzymes without interfering with the function of the gel. Future studies can also include embedding clinically relevant, traumatized neurons prepared with techniques reported by vandenPol et al.[105] within the gel and investigating cell-gel interaction, cell-cell interaction, and cell migration in three dimensions.

Although the study for G-C nanocomposites provides promising results, more in-depth works need to be done in the future. As implanted materials, the mechanical properties, of the film (e.g., contact stiffness, tensile strength, etc.) should be quantitatively measured and the biostability of the film needs to be determined under physiological conditions. The compositions and fabrications of free-standing films should also be optimized for the best neuron-material interaction. A study to determine the capability of G-C nanocomposite to electrically interface with neuron would be informative. Responses of other types of cells in the brain towards G-C films, such as astrocyte and microglia, should also be investigated. Finally, for practical applications, in vivo study should be conducted to investigate the host response to G-C nanocomposite.

REFERENCES

1. Rinaudo, M., Main properties and current applications of some polysaccharides as biomaterials. *Polymer International* **2008,** *57* (3), 397-430.

2. Domard, A.; Domard, M., *Chitosan: Structure-Properties Relationship and Biomedical Applications In Polymeric Biomaterials*. 2nd ed.; CRC Press: New York, 2002.

3. Sorlier, P.; Denuziere, A.; Viton, C.; Domard, A., Relation between the degree of acetylation and the electrostatic properties of chitin and chitosan. *Biomacromolecules* **2001,** *2* (3), 765-772.

4. Flory, P. J., *Principles of Polymer Chemistry*. Cornel University Press: Ithaca, New York, 1967.

5. Chenite, A.; Chaput, C.; Wang, D.; Combes, C.; Buschmann, M. D.; Hoemann, C. D.; Leroux, J. C.; Atkinson, B. L.; Binette, F.; Selmani, A., Novel injectable neutral solutions of chitosan form biodegradable gels in situ. *Biomaterials* **2000,** *21* (21), 2155-2161.

6. Crompton, K. E.; Goud, J. D.; Bellamkonda, R. V.; Gengenbach, T. R.; Finkelstein, D. I.; Horne, M. K.; Forsythe, J. S., Polylysine-functionalised thermoresponsive chitosan hydrogel for neural tissue engineering. *Biomaterials* **2007,** *28* (3), 441-449.

7. Cho, M. H.; Kim, K. S.; Ahn, H. H.; Kim, M. S.; Kim, S. H.; Khang, G.; Lee, B.; Lee, H. B., Chitosan gel as an in situ-forming scaffold for rat bone marrow mesenchymal stem cells in vivo. *Tissue Engineering Part A* **2008,** *14* (6), 1099-1108.

8. Chiu, Y. L.; Chen, S. C.; Su, C. J.; Hsiao, C. W.; Chen, Y. M.; Chen, H. L.; Sung, H. W., pH-triggered injectable hydrogels prepared from aqueous N-palmitoyl chitosan: In vitro characteristics and in vivo biocompatibility. *Biomaterials* **2009,** *30* (28), 4877-4888.

9. Tan, H. P.; Chu, C. R.; Payne, K. A.; Marra, K. G., Injectable in situ forming biodegradable chitosan-hyaluronic acid based hydrogels for cartilage tissue engineering. *Biomaterials* **2009,** *30* (13), 2499-2506.

10. Freier, T.; Koh, H. S.; Kazazian, K.; Shoichet, M. S., Controlling cell adhesion and degradation of chitosan films by N-acetylation. *Biomaterials* **2005,** *26* (29), 5872-5878.

11. Xu, G.; Nie, D. Y.; Wang, W. Z.; Zhang, P. H.; Shen, J.; Ang, B. T.; Liu, G. H.; Luo, X. G.; Chen, N. L.; Xiao, Z. C., Optic nerve regeneration in polyglycolic acid-chitosan conduits coated with recombinant L1-Fc. *Neuroreport* **2004,** *15* (14), 2167-2172.

12. Gan, Q.; Wang, T.; Cochrane, C.; McCarron, P., Modulation of surface charge, particle size and morphological properties of chitosan-TPP nanoparticles intended for gene delivery. *Colloids and Surfaces B-Biointerfaces* **2005,** *44* (2-3), 65-73.

13. Berthold, A.; Cremer, K.; Kreuter, J., Preparation and characterization of chitosan microspheres as drug carrier for prednisolone sodium phosphate as model for antiinflammatory drugs. *Journal of Controlled Release* **1996,** *39* (1), 17-25.

14. Calvo, P.; RemunanLopez, C.; VilaJato, J. L.; Alonso, M. J., Novel hydrophilic chitosan-polyethylene oxide nanoparticles as protein carriers. *Journal of Applied Polymer Science* **1997,** *63* (1), 125-132.

15. Grenha, A.; Seijo, B.; Serra, C.; Remunan-Lopez, C., Chitosan nanoparticle-loaded mannitol microspheres: Structure and surface characterization. *Biomacromolecules* **2007,** *8* (7), 2072-2079.

16. http://en.wikipedia.org/wiki/Neural_engineering.

17. http://www.ninds.nih.gov.

18. Reichert, W. M., *Indwelling Neural Implants: Strategies for Contending with the In Vivo Environment*. CRC Press: Boca Raton, 2008.

19. Orive, G.; Anitua, E.; Pedraz, J. L.; Emerich, D. F., Biomaterials for promoting brain protection, repair and regeneration. *Nature Reviews Neuroscience* **2009,** *10* (9), 682-U47.

20. Flanagan, L. A.; Ju, Y. E.; Marg, B.; Osterfield, M.; Janmey, P. A., Neurite branching on deformable substrates. *Neuroreport* **2002,** *13* (18), 2411-2415.

21. Nisbet, D. R.; Crompton, K. E.; Horne, M. K.; Finkelstein, D. I.; Forsythe, J. S., Neural tissue engineering of the CNS using hydrogels. *Journal of Biomedical Materials Research Part B-Applied Biomaterials* **2008,** *87B* (1), 251-263.

22. Bellamkonda, R.; Ranieri, J. P.; Aebischer, P., LAMININ OLIGOPEPTIDE DERIVATIZED AGAROSE GELS ALLOW 3-DIMENSIONAL NEURITE EXTENSION IN-VITRO. *Journal of Neuroscience Research* **1995,** *41* (4), 501-509.

23. Yu, X. J.; Dillon, G. P.; Bellamkonda, R. V., A laminin and nerve growth factor-laden three-dimensional scaffold for enhanced neurite extension. *Tissue Engineering* **1999,** *5* (4), 291-304.

24. Tian, W. M.; Hou, S. P.; Ma, J.; Zhang, C. L.; Xu, Q. Y.; Lee, I. S.; Li, H. D.; Spector, M.; Cui, F. Z., Hyaluronic acid-poly-D-lysine-based three-dimensional hydrogel for traumatic brain injury. *Tissue Engineering* **2005,** *11* (3-4), 513-525.

25. http://www.umich.edu/news/index.html?Releases/2006/Feb06/r020606a.

26. Lebedev, M. A.; Nicolelis, M. A. L., Brain-machine interfaces: past, present and future. *Trends in Neurosciences* **2006,** *29* (9), 536-546.

27. Normann, R. A., Technology Insight: future neuroprosthetic therapies for disorders of the nervous system. *Nature Clinical Practice Neurology* **2007,** *3* (8), 444-452.

28. Zielinska, E., Of Cells and Wires The first step to computer augmentation and neuroprosthetics lies in the connection between nerve cell and metal. How are scientists bridging the gap? *Scientist* **2009,** *23* (1), 32-37.

29. Nicolelis, M. A. L.; Dimitrov, D.; Carmena, J. M.; Crist, R.; Lehew, G.; Kralik, J. D.; Wise, S. P., Chronic, multisite, multielectrode recordings in macaque monkeys. *Proceedings of the National Academy of Sciences of the United States of America* **2003,** *100* (19), 11041-11046.

30. Kipke, D. R.; Vetter, R. J.; Williams, J. C.; Hetke, J. F., Silicon-substrate intracortical microelectrode arrays for long-term recording of neuronal spike activity in cerebral cortex. *Ieee Transactions on Neural Systems and Rehabilitation Engineering* **2003,** *11* (2), 151-155.

31. Rousche, P. J.; Normann, R. A., Chronic recording capability of the Utah Intracortical Electrode Array in cat sensory cortex. *Journal of Neuroscience Methods* **1998,** *82* (1), 1-15.

32. Bai, Q.; Wise, K. D., Single-unit neural recording with active microelectrode arrays. *Ieee Transactions on Biomedical Engineering* **2001,** *48* (8), 911-920.

33. Polikov, V. S.; Tresco, P. A.; Reichert, W. M., Response of brain tissue to chronically implanted neural electrodes. *Journal of Neuroscience Methods* **2005,** *148* (1), 1-18.

34. Williams, J. C.; Rennaker, R. L.; Kipke, D. R., Long-term neural recording characteristics of wire microelectrode arrays implanted in cerebral cortex. *Brain Research Protocols* **1999,** *4* (3), 303-313.

35. Seymour, J. P.; Kipke, D. R., Neural probe design for reduced tissue encapsulation in CNS. *Biomaterials* **2007,** *28* (25), 3594-3607.

36. Ignatius, M. J.; Sawhney, N.; Gupta, A.; Thibadeau, B. M.; Monteiro, O. R.; Brown, I. G., Bioactive surface coatings for nanoscale instruments: Effects on CNS neurons. *Journal of Biomedical Materials Research* **1998,** *40* (2), 264-274.

37. Kam, L.; Shain, W.; Turner, J. N.; Bizios, R., Selective adhesion of astrocytes to surfaces modified with immobilized peptides. *Biomaterials* **2002,** *23* (2), 511-515.

38. Cui, X. Y.; Lee, V. A.; Raphael, Y.; Wiler, J. A.; Hetke, J. F.; Anderson, D. J.; Martin, D. C., Surface modification of neural recording electrodes with conducting polymer/biomolecule blends. *Journal of Biomedical Materials Research* **2001,** *56* (2), 261-272.

39. Cui, X. Y.; Martin, D. C., Fuzzy gold electrodes for lowering impedance and improving adhesion with electrodeposited conducting polymer films. *Sensors and Actuators a-Physical* **2003,** *103* (3), 384-394.

40. Yang, J. Y.; Martin, D. C., Microporous conducting polymers on neural microelectrode arrays II. Physical characterization. *Sensors and Actuators a-Physical* **2004,** *113* (2), 204-211.

41. Ludwig, K. A.; Uram, J. D.; Yang, J. Y.; Martin, D. C.; Kipke, D. R., Chronic neural recordings using silicon microelectrode arrays electrochemically deposited with a poly(3,4-ethylenedioxythiophene) (PEDOT) film. *Journal of Neural Engineering* **2006,** *3* (1), 59-70.

42. Kennedy, P. R., THE CONE ELECTRODE - A LONG-TERM ELECTRODE THAT RECORDS FROM NEURITES GROWN ONTO ITS RECORDING SURFACE. *Journal of Neuroscience Methods* **1989,** *29* (3), 181-193.

43. Maynard, E. M.; Fernandez, E.; Normann, R. A., A technique to prevent dural adhesions to chronically implanted microelectrode arrays. *Journal of Neuroscience Methods* **2000,** *97* (2), 93-101.

44. Shain, W.; Spataro, L.; Dilgen, J.; Haverstick, K.; Retterer, S.; Isaacson, M.; Saltzman, M.; Turner, J. N., Controlling cellular reactive responses around neural prosthetic devices using peripheral and local intervention strategies. *Ieee Transactions on Neural Systems and Rehabilitation Engineering* **2003,** *11* (2), 186-188.

45. Tikka, T.; Fiebich, B. L.; Goldsteins, G.; Keinanen, R.; Koistinaho, J., Minocycline, a tetracycline derivative, is neuroprotective against excitotoxicity by inhibiting activation and proliferation of microglia. *Journal of Neuroscience* **2001,** *21* (8), 2580-2588.

46. Tikka, T. M.; Koistinaho, J. E., Minocycline provides neuroprotection against N-methyl-D-aspartate neurotoxicity by inhibiting microglia. *Journal of Immunology* **2001,** *166* (12), 7527-7533.

47. Rennaker, R. L.; Miller, J.; Tang, H.; Wilson, D. A., Minocycline increases quality and longevity of chronic neural recordings. *Journal of Neural Engineering* **2007,** *4* (2), L1-L5.

48. Kotov, N. A.; Winter, J. O.; Clements, I. P.; Jan, E.; Timko, B. P.; Campidelli, S.; Pathak, S.; Mazzatenta, A.; Lieber, C. M.; Prato, M.; Bellamkonda, R. V.; Silva, G. A.; Kam, N. W. S.; Patolsky, F.; Ballerini, L., Nanomaterials for Neural Interfaces. *Advanced Materials* **2009,** *21* (40), 3970-4004.

49. Cheng, M. Y.; Gong, K.; Li, J. M.; Gong, Y. D.; Zhao, N. M.; Zhang, X. F., Surface modification and characterization of chitosan film blended with poly-L-lysine. *Journal of Biomaterials Applications* **2004,** *19* (1), 59-75.

50. Yu, L. M. Y.; Leipzig, N. D.; Shoichet, M. S., Promoting neuron adhesion and growth. *Materials Today* **2008,** *11* (5), 36-43.

51. Dodla, M. C.; Bellamkonda, R. V., Differences between the effect of anisotropic and isotropic laminin and nerve growth factor presenting scaffolds on nerve regeneration across long peripheral nerve gaps. *Biomaterials* **2008,** *29* (1), 33-46.

52. Levesque, S. G.; Shoichet, M. S., Synthesis of cell-adhesive dextran hydrogels and macroporous scaffolds. *Biomaterials* **2006,** *27* (30), 5277-5285.

53. Fan, Y. W.; Cui, F. Z.; Hou, S. P.; Xu, Q. Y.; Chen, L. N.; Lee, I. S., Culture of neural cells on silicon wafers with nano-scale surface topograph. *Journal of Neuroscience Methods* **2002,** *120* (1), 17-23.

54. Foley, J. D.; Grunwald, E. W.; Nealey, P. F.; Murphy, C. J., Cooperative modulation of neuritogenesis by PC12 cells by topography and nerve growth factor. *Biomaterials* **2005,** *26* (17), 3639-3644.

55. Johansson, F.; Carlberg, P.; Danielsen, N.; Montelius, L.; Kanje, M., Axonal outgrowth on nano-imprinted patterns. *Biomaterials* **2006,** *27* (8), 1251-1258.

56. Dillon, G. P.; Yu, X. J.; Bellamkonda, R. V., The polarity and magnitude of ambient charge influences three-dimensional neurite extension from DRGs. *Journal of Biomedical Materials Research* **2000,** *51* (3), 510-519.

57. Chatelet, C.; Damour, O.; Domard, A., Influence of the degree of acetylation on some biological properties of chitosan films. *Biomaterials* **2001,** *22* (3), 261-268.

58. Cao, W. L.; Jing, D. H.; Li, J. M.; Gong, Y. D.; Zhao, N. M.; Zhang, X. F., Effects of the degree of deacetylation on the physicochemical properties and Schwann cell affinity of chitosan films. *Journal of Biomaterials Applications* **2005,** *20* (2), 157-177.

59. Arnott, S.; Fulmer, A.; Scott, W. E.; Dea, I. C. M.; Moorhouse, R.; Rees, D. A., AGAROSE DOUBLE HELIX AND ITS FUNCTION IN AGAROSE-GEL STRUCTURE. *Journal of Molecular Biology* **1974,** *90* (2), 269-&.

60. Dillon, G. P.; Yu, X. J.; Sridharan, A.; Ranieri, J. P.; Bellamkonda, R. V., The influence of physical structure and charge on neurite extension in a 3D hydrogel scaffold. *Journal of Biomaterials Science-Polymer Edition* **1998,** *9* (10), 1049-1069.

61. Martin, B. C.; Minner, E. J.; Wiseman, S. L.; Klank, R. L.; Gilbert, R. J., Agarose and methylcellulose hydrogel blends for nerve regeneration applications. *Journal of Neural Engineering* **2008,** *5* (2), 221-231.

62. Lin, P. W.; Wu, C. C.; Chen, C. H.; Ho, H. O.; Chen, Y. C.; Sheu, M. T., Characterization of cortical neuron outgrowth in two- and three-dimensional culture systems. *Journal of Biomedical Materials Research Part B-Applied Biomaterials* **2005,** *75B* (1), 146-157.

63. Balgude, A. P.; Yu, X.; Szymanski, A.; Bellamkonda, R. V., Agarose gel stiffness determines rate of DRG neurite extension in 3D cultures. *Biomaterials* **2001,** *22* (10), 1077-1084.

64. Hanson, G. R.; Iversen, P. L.; Partlow, L. M., PREPARATION AND PARTIAL CHARACTERIZATION OF HIGHLY PURIFIED PRIMARY CULTURES OF NEURONS AND NONNEURONAL (GLIAL) CELLS FROM EMBRYONIC CHICK CEREBRAL HEMISPHERES AND SEVERAL OTHER REGIONS OF THE NERVOUS-SYSTEM. *Dev. Brain Res.* **1982,** *3* (4), 529-545.

65. www.olympusfluoview.com.

66. Radio, N. M.; Mundy, W. R., Developmental neurotoxicity testing in vitro: Models for assessing chemical effects on neurite outgrowth. *Neurotoxicology* **2008,** *29* (3), 361-376.

67. Kligman, D., NEURITE OUTGROWTH FROM CEREBRAL CORTICAL-NEURONS IS PROMOTED BY MEDIUM CONDITIONED OVER HEART-CELLS. *Journal of Neuroscience Research* **1982,** *8* (2-3), 281-287.

68. Yeung, T.; Georges, P. C.; Flanagan, L. A.; Marg, B.; Ortiz, M.; Funaki, M.; Zahir, N.; Ming, W. Y.; Weaver, V.; Janmey, P. A., Effects of substrate stiffness on cell morphology, cytoskeletal structure, and adhesion. *Cell Motility and the Cytoskeleton* **2005,** *60* (1), 24-34.

69. Discher, D. E.; Janmey, P.; Wang, Y. L., Tissue cells feel and respond to the stiffness of their substrate. *Science* **2005,** *310* (5751), 1139-1143.

70. Levental, I.; Georges, P. C.; Janmey, P. A., Soft biological materials and their impact on cell function. *Soft Matter* **2007,** *3* (3), 299-306.

71. Clark, A. H.; Richardson, R. K.; Rossmurphy, S. B.; Stubbs, J. M., Structural and Mechanical-Properties of Agar Gelatin Co-Gels - Small-Deformation Studies. *Macromolecules* **1983,** *16* (8), 1367-1374.

72. Lee, N. K.; Obukhov, S., Collapse dynamics of a polyelectrolyte. *Europhysics Letters* **2004,** *66* (3), 350-356.

73. Rezania, A.; Healy, K. E., The effect of peptide surface density on mineralization of a matrix deposited by osteogenic cells. *Journal of Biomedical Materials Research* **2000,** *52* (4), 595-600.

74. Clark, P.; Britland, S.; Connolly, P., GROWTH CONE GUIDANCE AND NEURON MORPHOLOGY ON MICROPATTERNED LAMININ SURFACES. *Journal of Cell Science* **1993,** *105*, 203-212.

75. Schense, J. C.; Hubbell, J. A., Three-dimensional migration of neurites is mediated by adhesion site density and affinity. *Journal of Biological Chemistry* **2000,** *275* (10), 6813-6818.

76. Labrador, R. O.; Buti, M.; Navarro, X., PERIPHERAL-NERVE REPAIR - ROLE OF AGAROSE MATRIX DENSITY ON FUNCTIONAL RECOVERY. *Neuroreport* **1995,** *6* (15), 2022-2026.

77. Donoghue, J. P., Connecting cortex to machines: recent advances in brain interfaces. *Nature Neuroscience* **2002,** *5*, 1085-1088.

78. Grill, W. M.; Norman, S. E.; Bellamkonda, R. V., Implanted Neural Interfaces: Biochallenges and Engineered Solutions. *Annual Review of Biomedical Engineering* **2009,** *11*, 1-24.

79. Hochberg, L. R.; Serruya, M. D.; Friehs, G. M.; Mukand, J. A.; Saleh, M.; Caplan, A. H.; Branner, A.; Chen, D.; Penn, R. D.; Donoghue, J. P., Neuronal ensemble control of prosthetic devices by a human with tetraplegia. *Nature* **2006,** *442* (7099), 164-171.

80. Kipke, D. R.; Shain, W.; Buzsaki, G.; Fetz, E.; Henderson, J. M.; Hetke, J. F.; Schalk, G., Advanced Neurotechnologies for Chronic Neural Interfaces: New Horizons and Clinical Opportunities. *Journal of Neuroscience* **2008,** *28* (46), 11830-11838.

81. Nicolelis, M. A. L., Actions from thoughts. *Nature* **2001,** *409* (6818), 403-407.

82. Schwartz, A. B., Cortical neural prosthetics. *Annual Review of Neuroscience* **2004,** *27*, 487-507.

83. Novoselov, K. S.; Geim, A. K.; Morozov, S. V.; Jiang, D.; Zhang, Y.; Dubonos, S. V.; Grigorieva, I. V.; Firsov, A. A., Electric Field Effect in Atomically Thin Carbon Films. *Science* **2004,** *306* (5696), 666-669.

84. Bolotin, K. I.; Sikes, K. J.; Jiang, Z.; Klima, M.; Fudenberg, G.; Hone, J.; Kim, P.; Stormer, H. L., Ultrahigh electron mobility in suspended graphene. *Solid State Communications* **2008,** *146* (9-10), 351-355.

85. Balandin, A. A.; Ghosh, S.; Bao, W. Z.; Calizo, I.; Teweldebrhan, D.; Miao, F.; Lau, C. N., Superior thermal conductivity of single-layer graphene. *Nano Letters* **2008,** *8* (3), 902-907.

86. Stoller, M. D.; Park, S. J.; Zhu, Y. W.; An, J. H.; Ruoff, R. S., Graphene-Based Ultracapacitors. *Nano Letters* **2008,** *8* (10), 3498-3502.

87. Stankovich, S.; Dikin, D. A.; Dommett, G. H. B.; Kohlhaas, K. M.; Zimney, E. J.; Stach, E. A.; Piner, R. D.; Nguyen, S. T.; Ruoff, R. S., Graphene-based composite materials. *Nature* **2006,** *442* (7100), 282-286.

88. Ramanathan, T.; Abdala, A. A.; Stankovich, S.; Dikin, D. A.; Herrera-Alonso, M.; Piner, R. D.; Adamson, D. H.; Schniepp, H. C.; Chen, X.; Ruoff, R. S.; Nguyen, S. T.; Aksay, I. A.; Prud'homme, R. K.; Brinson, L. C., Functionalized graphene sheets for polymer nanocomposites. *Nature Nanotechnology* **2008,** *3* (6), 327-331.

89. Blake, P.; Brimicombe, P. D.; Nair, R. R.; Booth, T. J.; Jiang, D.; Schedin, F.; Ponomarenko, L. A.; Morozov, S. V.; Gleeson, H. F.; Hill, E. W.; Geim, A. K.; Novoselov, K. S., Graphene-based liquid crystal device. *Nano Letters* **2008,** *8* (6), 1704-1708.

90. Chen, H.; Muller, M. B.; Gilmore, K. J.; Wallace, G. G.; Li, D., Mechanically strong, electrically conductive, and biocompatible graphene paper. *Advanced Materials* **2008,** *20* (18), 3557-+.

91. Agarwal, S.; Zhou, X. Z.; Ye, F.; He, Q. Y.; Chen, G. C. K.; Soo, J.; Boey, F.; Zhang, H.; Chen, P., Interfacing Live Cells with Nanocarbon Substrates. *Langmuir* **2010,** *26* (4), 2244-2247.

92. Worle-Knirsch, J. M.; Pulskamp, K.; Krug, H. F., Oops they did it again! Carbon nanotubes hoax scientists in viability assays. *Nano Letters* **2006,** *6* (6), 1261-1268.

93. Monteiro-Riviere, N. A.; Nemanich, R. J.; Inman, A. O.; Wang, Y. Y. Y.; Riviere, J. E., Multi-walled carbon nanotube interactions with human epidermal keratinocytes. *Toxicology Letters* **2005,** *155* (3), 377-384.

94. Pantarotto, D.; Briand, J. P.; Prato, M.; Bianco, A., Translocation of bioactive peptides across cell membranes by carbon nanotubes. *Chemical Communications* **2004,** (1), 16-17.

95. Pantarotto, D.; Singh, R.; McCarthy, D.; Erhardt, M.; Briand, J. P.; Prato, M.; Kostarelos, K.; Bianco, A., Functionalized carbon nanotubes for plasmid DNA gene delivery. *Angewandte Chemie-International Edition* **2004,** *43* (39), 5242-5246.

96. Helland, A.; Wick, P.; Koehler, A.; Schmid, K.; Som, C., Reviewing the environmental and human health knowledge base of carbon nanotubes. *Environmental Health Perspectives* **2007,** *115* (8), 1125-1131.

97. Kagan, V. E.; Tyurina, Y. Y.; Tyurin, V. A.; Konduru, N. V.; Potapovich, A. I.; Osipov, A. N.; Kisin, E. R.; Schwegler-Berry, D.; Mercer, R.; Castranova, V.; Shvedova, A. A., Direct and indirect effects of single walled carbon nanotubes on RAW 264.7 macrophages: Role of iron. *Toxicology Letters* **2006,** *165* (1), 88-100.

98. Tian, F. R.; Cui, D. X.; Schwarz, H.; Estrada, G. G.; Kobayashi, H., Cytotoxicity of single-wall carbon nanotubes on human fibroblasts. *Toxicology in Vitro* **2006,** *20* (7), 1202-1212.

99. Si, Y.; Samulski, E. T., Synthesis of water soluble graphene. *Nano Letters* **2008,** *8* (6), 1679-1682.

100. Park, S.; Ruoff, R. S., Chemical methods for the production of graphenes. *Nature Nanotechnology* **2009,** *4* (4), 217-224.

101. Castner, D. G.; Ratner, B. D., Biomedical surface science: Foundations to frontiers. *Surface Science* **2002,** *500* (1-3), 28-60.

102. Lee, H.; Bellamkonda, R. V.; Sun, W.; Levenston, M. E., Biomechanical analysis of silicon microelectrode-induced strain in the brain. *J Neural Eng* **2005,** *2* (4), 81-9.

103. Subbaroyan, J.; Martin, D. C.; Kipke, D. R., A finite-element model of the mechanical effects of implantable microelectrodes in the cerebral cortex. *J Neural Eng* **2005,** *2* (4), 103-13.

104. Flemming, R. G.; Murphy, C. J.; Abrams, G. A.; Goodman, S. L.; Nealey, P. F., Effects of synthetic micro- and nano-structured surfaces on cell behavior. *Biomaterials* **1999,** *20* (6), 573-588.

105. vandenPol, A. N.; Obrietan, K.; Chen, G., Excitatory actions of GABA after neuronal trauma. *Journal of Neuroscience* **1996,** *16* (13), 4283-4292.

VITA

Zheng Cao was born in Beijing, China on March 26, 1984. She received her bachelor's degree in Materials Science and Engineering from Tsinghua University in July of 2006. After graduation from Tsinghua University, she has been working as a product engineer in Samsung Electro-Mechanics, Tianjin, China for one year. In August of 2008, she entered University of Tennessee, Knoxville to pursue advanced degree in Polymer Engineering. She received her Master degree in May of 2010.